



## RESEARCH ARTICLE

10.1002/2016GB005460

## Key Points:

- Anthropogenic CO<sub>2</sub> accumulation rate was estimated based on measured change in ocean δ<sup>13</sup>C between the 1990s and 2000s
- Net anthropogenic CO<sub>2</sub> uptake rates independent of ΔpCO<sub>2</sub> were estimated from measured δ<sup>13</sup>C changes
- Regional differences between anthropogenic DIC<sup>13</sup> accumulation and air-sea <sup>13</sup>CO<sub>2</sub> flux rates indicate importance of ocean transport

## Correspondence to:

P. Quay,  
pdquay@uw.edu

## Citation:

Quay, P., R. Sonnerup, D. Munro, and C. Sweeney (2017), Anthropogenic CO<sub>2</sub> accumulation and uptake rates in the Pacific Ocean based on changes in the <sup>13</sup>C/<sup>12</sup>C of dissolved inorganic carbon, *Global Biogeochem. Cycles*, 31, 59–80, doi:10.1002/2016GB005460.

Received 8 JUN 2016

Accepted 12 DEC 2016

Accepted article online 14 DEC 2016

Published online 13 JAN 2017

## Anthropogenic CO<sub>2</sub> accumulation and uptake rates in the Pacific Ocean based on changes in the <sup>13</sup>C/<sup>12</sup>C of dissolved inorganic carbon

P. Quay<sup>1</sup> , R. Sonnerup<sup>1,2</sup>, D. Munro<sup>3</sup> , and C. Sweeney<sup>4</sup>

<sup>1</sup>School of Oceanography, University of Washington, Seattle, Washington, USA, <sup>2</sup>Joint Institute for Study of the Atmosphere and Ocean, University of Washington, Seattle, Washington, USA, <sup>3</sup>Department of Atmospheric and Oceanic Sciences and Institute of Arctic and Alpine Research, University of Colorado Boulder, Boulder, Colorado, USA, <sup>4</sup>Cooperative Institute for Research in Environmental Sciences, University of Colorado and NOAA Earth System Research Laboratory, Boulder, Colorado, USA

**Abstract** The anthropogenic CO<sub>2</sub> accumulation rate for the Pacific Ocean was estimated from the decrease in δ<sup>13</sup>C of the dissolved inorganic carbon measured on six World Ocean Circulation Experiment cruises during the 1990s and repeated during Climate Variability and Predictability in the 2000s. A mean depth-integrated anthropogenic δ<sup>13</sup>C change of  $-83 \pm 20\text{‰ m decade}^{-1}$  was estimated for the basin by using the multiple linear regression approach. The largest anthropogenic δ<sup>13</sup>C decreases occurred between 40°S and 60°S, whereas the smallest decreases occurred in the Southern Ocean and subpolar North Pacific. A mean anthropogenic CO<sub>2</sub> accumulation rate of  $0.41 \pm 0.13 \text{ mol C m}^{-2} \text{ yr}^{-1}$  ( $0.82 \pm 0.26 \text{ Pg C yr}^{-1}$ ) was determined based on observed δ<sup>13</sup>C changes and is in agreement with previous observation- and model-based estimates. The mean dissolved inorganic carbon DIC<sup>13</sup> inventory change of  $-178 \pm 43\text{‰ mol m}^{-2} \text{ decade}^{-1}$  was primarily the result of air-sea CO<sub>2</sub> exchange acting on the measured air-sea δ<sup>13</sup>C disequilibrium of  $\sim -1.2 \pm 0.1\text{‰}$ . Regional differences between the DIC<sup>13</sup> inventory change and air-sea <sup>13</sup>CO<sub>2</sub> flux yielded net anthropogenic CO<sub>2</sub> uptake rates (independent of ΔpCO<sub>2</sub>) that ranged from  $\sim 0$  to  $1 \text{ mol m}^{-2} \text{ yr}^{-1}$  and basin-wide mean of  $1.2 \pm 1.5 \text{ Pg C yr}^{-1}$ . High rates of surface ocean DIC increase and δ<sup>13</sup>C decrease observed in the Drake Passage (53°S–60°S) support above average anthropogenic CO<sub>2</sub> accumulation since 2005. Observed δ<sup>13</sup>C changes in the Pacific Ocean indicate that ocean transport significantly impacted the anthropogenic CO<sub>2</sub> distribution and illustrate the utility of δ<sup>13</sup>C as a tracer to unravel the processes controlling the present and future accumulation of anthropogenic CO<sub>2</sub> in the ocean.

### 1. Introduction

The accumulation of anthropogenic CO<sub>2</sub> in the ocean is a key process affecting future atmospheric CO<sub>2</sub>. Anthropogenic CO<sub>2</sub> accumulation rates in the ocean since the 1990s have been estimated by using increases in dissolved inorganic carbon (DIC) concentration measured along cruise tracks occupied during World Ocean Circulation Experiment (WOCE) (1990s) and Climate Variability and Predictability (CLIVAR)-Repeat Hydrography (2000s) programs [Sabine and Tanhua, 2010]. Most CO<sub>2</sub> accumulation rate estimates require techniques to extract a small anthropogenic DIC change ( $\sim 10 \mu\text{mol kg}^{-1} \text{ decade}^{-1}$ ) from a large ( $\sim 2100 \mu\text{mol kg}^{-1}$ ) and variable ( $\sim 200 \text{ mol kg}^{-1}$ ) background DIC concentration. The use of multiple linear correlations with concurrent nutrient, oxygen, and hydrographic data (the Multiple Linear Regression or MLR approach) has yielded DIC accumulation rates that can range regionally by more than an order of magnitude from  $\sim 0.1$  to  $3 \text{ mol m}^{-2} \text{ yr}^{-1}$  [Sabine et al., 2008], where an average CO<sub>2</sub> accumulation rate of  $0.53 \text{ mol m}^{-2} \text{ yr}^{-1}$  corresponds to  $\sim 2.2 \text{ Pg yr}^{-1}$  of global ocean uptake. Because anthropogenic CO<sub>2</sub> accumulation rates estimated from measured DIC change are limited primarily to the cruise tracks occupied during WOCE and CLIVAR, global ocean CO<sub>2</sub> uptake rates are often estimated from models or global distributions of tracer analogs of anthropogenic CO<sub>2</sub> [e.g., Gruber et al., 2009; Khatiwala et al., 2013]. The tracer- and model-based estimates on which current Intergovernmental Panel on Climate Change estimates are based yield global ocean CO<sub>2</sub> uptake rates of  $2.0$  to  $2.2 \text{ mol m}^{-2} \text{ yr}^{-1}$  for the 1990s and 2000s, respectively. There is a continued need to validate these model- and tracer-based uptake rates at regional scales as is done in this study.

Anthropogenic CO<sub>2</sub> accumulation rates have been estimated by applying the MLR approach to measured decadal changes in the <sup>13</sup>C/<sup>12</sup>C of DIC (referred to here as δ<sup>13</sup>C) in the ocean [e.g., *Sonnerup et al.*, 2000; *McNeil et al.*, 2001; *Quay et al.*, 2007; *Ko et al.*, 2014]. δ<sup>13</sup>C is a useful tracer of anthropogenic CO<sub>2</sub> changes because the industrial era decrease in δ<sup>13</sup>C is caused by the anthropogenic CO<sub>2</sub> increase [*Körtzinger et al.*, 2003] and the ability to detect an anthropogenic δ<sup>13</sup>C change in the ocean is greater than for DIC itself [*Quay et al.*, 2003]. In addition, the air-sea <sup>13</sup>CO<sub>2</sub> flux can be well determined because unlike the air-sea CO<sub>2</sub> flux, the δ<sup>13</sup>C gradient across the air-sea interface is large relative to its variability and is more accurately determined with limited measurements [*Quay et al.*, 2007]. A comparison of the DIC<sup>13</sup> inventory change rate to air-sea <sup>13</sup>CO<sub>2</sub> flux can identify ocean regions where transport is exporting or importing anthropogenic CO<sub>2</sub>. For example, in the North Atlantic Ocean the measured DIC<sup>13</sup> inventory change rate was twice the air-sea <sup>13</sup>CO<sub>2</sub> flux rate between the 1990s and 2000s, which indicated that the meridional overturning circulation significantly contributed to anthropogenic CO<sub>2</sub> accumulation [*Quay et al.*, 2007].

In this study, the DIC<sup>13</sup> inventory change for the Pacific Ocean between the 1990s and 2000s was estimated by using a MLR-based analysis of δ<sup>13</sup>C measurements during six WOCE/CLIVAR cruises that spanned the entire north-south and east-west extent of the Pacific Ocean. Additionally, decade-long δ<sup>13</sup>C time series measurements of surface ocean change are presented for the subtropical North Pacific and Drake Passage. The air-sea <sup>13</sup>CO<sub>2</sub> flux was estimated based on ~2750 surface δ<sup>13</sup>C measurements obtained from WOCE/CLIVAR cruises and volunteer-observing ships. These δ<sup>13</sup>C data sets demonstrate the utility of using δ<sup>13</sup>C as a tracer of anthropogenic CO<sub>2</sub> uptake and redistribution in the Pacific Ocean.

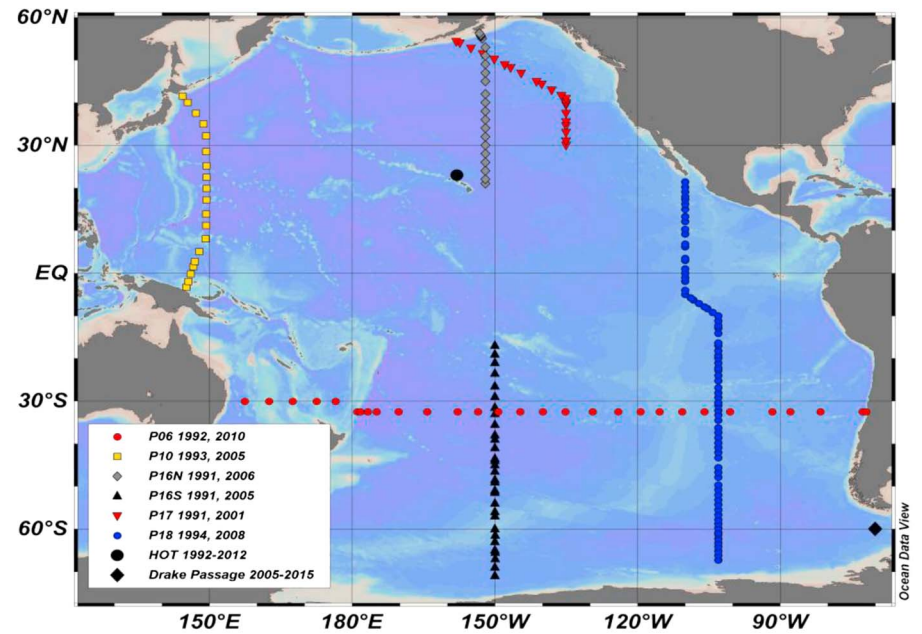
## 2. Methodology

### 2.1. Data Sets

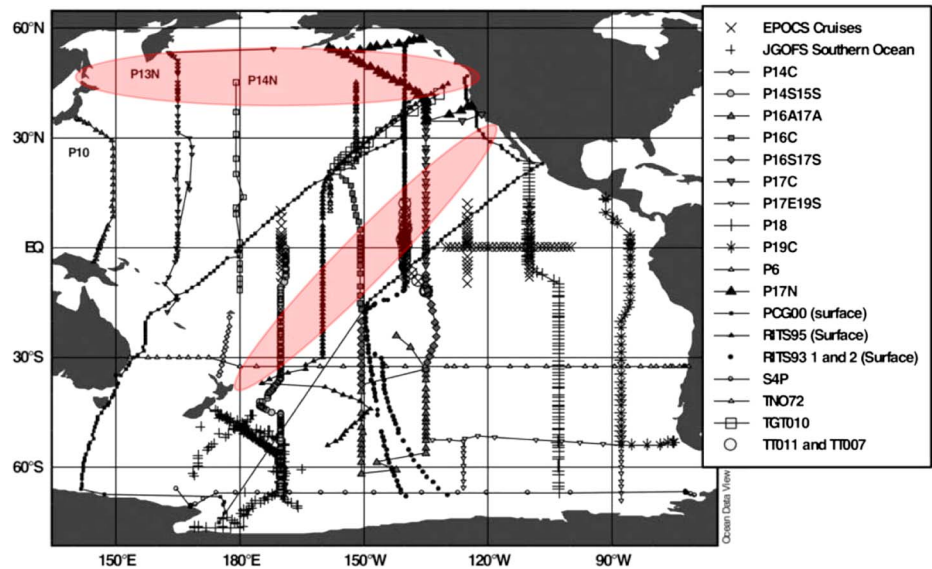
The δ<sup>13</sup>C ocean inventory change between the 1990s and 2000s was determined by using data from several WOCE and CLIVAR cruises that span the Pacific Ocean (Figure 1). Here δ<sup>13</sup>C represents the δ<sup>13</sup>C of DIC where  $\delta^{13}\text{C} (\text{‰}) = [(^{13}\text{C}/^{12}\text{C})_{\text{sample}} / (^{13}\text{C}/^{12}\text{C})_{\text{standard}} - 1] \cdot 1000$  and the standard is Pee-Dee belemnite. Specifically, the cruises included P06, P10, P16N, P16S, P17N, and P18 with the cruise locations (Figure 1) and data set characteristics presented in Table 1. There were a total of 127 station locations where δ<sup>13</sup>C was measured during both WOCE and CLIVAR cruises and data analyzed by the MLR method to estimate the magnitude of the anthropogenic δ<sup>13</sup>C (and DIC) changes (see Table S1).

Additionally, surface ocean δ<sup>13</sup>C time series measurements at the Hawaii Ocean Time-Series site (HOT; 23°N, 158°W) [*Karl and Lukas*, 1996] between 1991 and 2012 (*n* = 516) and at the Drake Passage Time Series (55°S–63°S and 68°W–58°W) [*Munro et al.*, 2015] between 2005 and 2015 (*n* = 768) were included to obtain a more detailed time history of the anthropogenic δ<sup>13</sup>C change in these regions. To more accurately determine the air-sea <sup>13</sup>CO<sub>2</sub> flux δ<sup>13</sup>C measurements for the surface ocean from two volunteer-observing (container) ship sampling programs (*n* = 990) in the tropical Pacific during 2004–2005 [*Quay et al.*, 2009] and in the North Pacific between 2008 and 2015 supplemented surface δ<sup>13</sup>C measurements (*n* ~ 1700) during WOCE and CLIVAR cruises (P06, P10, P14, P15, P16, P17, and P19) and other research cruises (e.g., JGOFS, EPOC, and RITS) in the Pacific during the 1990s and 2000, the latter of which were described previously [*Quay et al.*, 2003] (Figure 1).

Three laboratories measured δ<sup>13</sup>C of DIC during WOCE and CLIVAR: the National Ocean Sciences Accelerator Mass Spectrometry facility (NOSAMS), University of Washington (UW), and Japan Agency for Marine-Earth Science and Technology (JAMSTEC), while all the volunteer-observing ship and time series samples were measured at the UW. The typical δ<sup>13</sup>C measurement precision for these laboratories was ~ ±0.03‰ [*Quay et al.*, 2003]. However, an equivalent level of accuracy was significantly more difficult to attain; i.e., biases between laboratories and between cruises in the δ<sup>13</sup>C measurements have occurred [*Quay et al.*, 2003]. To estimate biases between δ<sup>13</sup>C measurements on the same cruise track between WOCE and CLIVAR the MLR method (described below) was used to determine δ<sup>13</sup>C residuals in the deep water (>2000 m) as discussed in *Quay et al.* [2007]. It was assumed that there has been no anthropogenic change in the δ<sup>13</sup>C below 2000 m in the Pacific Ocean between the 1990s and 2000s, and thus, any MLR-based δ<sup>13</sup>C residual calculated for the deep water between cruises was assumed to represent a measurement offset and a correction for this deep water δ<sup>13</sup>C offset was applied to the entire δ<sup>13</sup>C data set. The following were the corrections applied to



A



B

**Figure 1.** The locations of cruises where (a)  $\delta^{13}\text{C}$  data were analyzed by using the MLR method (P06, P10, P13, P16, P17, and P18) and the surface ocean  $\delta^{13}\text{C}$  time series at HOT (23°N, 158°W) (solid circle) and Drake Passage (~60°S, 65°W) (solid diamond). (b) Surface ocean  $\delta^{13}\text{C}$  was measured during 1990s and 2000s. The oval shapes represent the areal coverage of surface  $\delta^{13}\text{C}$  samples collected during container ship crossings between 2004 and 2012 (see text).

the WOCE  $\delta^{13}\text{C}$  data sets: 0.14‰ for P06, 0.04‰ for P10, 0.27‰ for P16S, 0.20‰ for P16N, 0.06‰ for P17N, and 0.00‰ for P18 (Table 1). Between cruise  $\delta^{13}\text{C}$  biases of up to 0.14‰ have been observed previously for modern ocean  $\delta^{13}\text{C}$  data sets [Quay *et al.*, 2003]. The  $\delta^{13}\text{C}$  offsets for WOCE P16S and P16N were outside the expected range and likely represent a methodological issue for these specific data sets. (Note that P16 in 1991 was the first WOCE cruise on which  $\delta^{13}\text{C}$  was measured.)

Because the MLR approach (described below) used temperature, salinity, oxygen, and nutrient data to estimate  $\delta^{13}\text{C}$ , any analytical offsets in these measurements between WOCE and CLIVAR cruises would bias

**Table 1.** Mean MLR Residuals for  $\delta^{13}\text{C}$  and DIC for the WOCE and CLIVAR Cruise Data Sets Analyzed in This Study<sup>a</sup>

Cruise	Location	Dates	Stations (No. of Samples)	$\delta^{13}\text{C}$ Res. (‰)	$\delta^{13}\text{C}$ Corr. (‰)	DIC Res. ( $\mu\text{mol kg}^{-1}$ )
P06	along ~32°S	1992	43 (905)	±0.09	0.14	±4
	150°E–80°W	2010	29 (641)	±0.05		±4
P10	along ~150°E	1993	35 (574)	±0.04	0.04	±3
	0°N–40°N	2005	19 (488)	±0.05		±4
P16N	along ~150°W	1991	18 (252)	±0.18	0.20	±4
	20°N–55°N	2006	42 (941)	±0.07		±3
P16S	along ~150°W	1991	27 (551)	±0.10	0.27	±6
	70°S–20°S	2005	22 (552)	±0.06		±4
P17N	along ~135°W	1993	28 (574)	±0.06	0.06	±7
	30°N–55°N	2001	21 (645)	±0.04		±2
P18	along 105°W	1994	32 (830)	±0.05	0.00	±4
	65°S–20°N	2008	24 (464)	±0.07		±3

<sup>a</sup> $\delta^{13}\text{C}$  correction applied to WOCE data set based on deep water offset between WOCE and CLIVAR cruises (as discussed in text). Location, date, station, and sample numbers are listed for each cruise.

the MLR results. Analytical corrections recommended by Global Ocean Data Analysis Project (GLODAP) [Key *et al.*, 2015; Olsen *et al.*, 2016] and/or Pacific Ocean Interior Carbon were applied to the temperature, salinity, dissolved  $\text{O}_2$ , nutrient, and DIC data before the MLR analyses [e.g., Sabine *et al.*, 2008]. Any unidentified offsets in these parameters between WOCE and CLIVAR cruises would have been incorporated into the calculated deep water MLR  $\delta^{13}\text{C}$  offsets.

## 2.2. Multiple Linear Regression (MLR) Approach

The MLR approach has been used extensively to estimate anthropogenic DIC and  $\delta^{13}\text{C}$  inventory change [e.g., Wallace, 1995; Sonnerup *et al.*, 2000; Sabine *et al.*, 2008]. It establishes concurrent linear correlations between the  $\delta^{13}\text{C}$  (or DIC) of seawater and measured properties of seawater and assumes that these relationships hold over time except for anthropogenic changes. Thus, a MLR estimate of  $\delta^{13}\text{C}$  as applied here was expressed as follows:

$$\delta^{13}\text{C} = \beta + m_1\theta + m_2S + m_3\text{AOU} + m_4\text{Nutrient} + R \quad (1)$$

where  $\beta$  represented the intercept,  $m_1$  through  $m_4$  represented the regression coefficients for each predictive variable,  $R$  represented the residuals between the predicted and observed  $\delta^{13}\text{C}$  for each data point,  $\theta$  was potential temperature,  $S$  was salinity, AOU was apparent oxygen utilization, and nutrient was either phosphate or nitrate. The MLR approach attempted to account for the portion of temporal and spatial variations in  $\delta^{13}\text{C}$  (and DIC) that resulted from changes in the hydrographic and biogeochemical characteristics of the water. The portion of the  $\delta^{13}\text{C}$  (and DIC) change not explained by the MLR (i.e., residuals) was assumed to result from the accumulation of anthropogenic  $\text{CO}_2$  during the time interval between cruises.

Typically, the MLR has been performed on two data sets collected along a single repeated WOCE/CLIVAR cruise track with the ocean  $\delta^{13}\text{C}$  (or DIC) data sets subdivided spatially or by density and MLRs performed on subsets of the data in order to improve the accuracy of the MLR predictions [e.g., Quay *et al.*, 2007; Sabine *et al.*, 2008]. For this study the  $\delta^{13}\text{C}$  and DIC data sets were sorted by density and an MLR was determined for each specified density interval following the procedure described by Quay *et al.* [2007] which allowed the MLR to correlate  $\delta^{13}\text{C}$  (and DIC) with spatial variations in the preformed  $\delta^{13}\text{C}$  (and DIC) and hydrographic properties in the outcrop regions where water masses subduct.

Typically, the individual MLR predicted the  $\delta^{13}\text{C}$  for a specific cruise data set to better than  $\pm 0.10\text{‰}$ , e.g.,  $\pm 0.04\text{‰}$  on A16 in North Atlantic [Quay *et al.*, 2007] and  $\pm 0.06\text{‰}$  on P18 in South Pacific [Ko *et al.*, 2014]. For the cruises reported here (P06, P10, P16, P17, and P18) the mean  $\delta^{13}\text{C}$  residuals ranged from  $\pm 0.04$  to  $0.10\text{‰}$  (Table 1) except for the WOCE P16N cruise (1991) where the residual was  $\pm 0.18\text{‰}$ , which may be related to a data quality issue (discussed above) and/or the small size of the  $\delta^{13}\text{C}$  data set ( $n = 252$ ). The mean MLR-based DIC residuals for these same cruises ranged from  $\pm 2$  to  $7 \mu\text{mol kg}^{-1}$  (Table 1) which agreed with previous MLR residual range of  $\pm 2$ – $7 \mu\text{mol kg}^{-1}$  observed on P16 and P02 by Sabine *et al.* [2008].

In this study, the extended or eMLR approach [Friis *et al.*, 2005] was used to estimate inventory changes in DIC and  $\delta^{13}\text{C}$ . The eMLR used the difference between MLR coefficients determined for the earlier and later cruise data sets to estimate the anthropogenic  $\delta^{13}\text{C}$  or DIC change, and thus, the residual represented a difference between two sets of predicted  $\delta^{13}\text{C}$  (or DIC) values. Generally, the eMLR approach smoothed the spatial or depth trends in the anthropogenic  $\delta^{13}\text{C}$  (or DIC) change by reducing individual measurement anomalies [Plancherel *et al.*, 2009]. The resulting coefficients and errors of the eMLR analysis of  $\delta^{13}\text{C}$  data for each cruise are presented in Table S2.

The ratio of the anthropogenic  $\delta^{13}\text{C}$  to DIC change has been referred to as RC [McNeil *et al.*, 2001]. RC was calculated from the eMLR-based estimates of anthropogenic  $\delta^{13}\text{C}$  and DIC residuals for each cruise. Additionally, values of RC for the surface ocean were determined directly from the decade-long  $\delta^{13}\text{C}$  and DIC time series measurements at HOT and Drake Passage. At both time series sites RC represented the slope ratio of MLR-based residuals for  $\delta^{13}\text{C}$  and DIC versus time in order to account for interannual changes in surface temperature, salinity, and nutrients.

### 2.3. Error Analysis

The uncertainty in the depth-integrated  $\delta^{13}\text{C}$  inventory changes determined by the eMLR method depended on the uncertainties in the fits of the MLR procedure to the  $\delta^{13}\text{C}$  measurements from the earlier and later cruise on each density surface. A Monte Carlo approach was used to randomly select a depth profile of  $\delta^{13}\text{C}$  residuals based on the mean and standard deviation (SD) of the residuals at each depth determined by the MLR procedure as described by Quay *et al.* [2007]. This procedure was performed for each station ( $n = 127$ ), and the typical uncertainty in the depth-integrated  $\delta^{13}\text{C}$  change was 10–20%. The mean and errors ( $\pm 1$  SD) in the depth-integrated  $\delta^{13}\text{C}$  depth profiles at each station pair analyzed are presented in Table S1.

Possible spatial biases in the  $\delta^{13}\text{C}$  data set were evaluated. Mean basin-wide depth-integrated  $\delta^{13}\text{C}$  changes were determined by averaging the changes determined for individual stations over  $10^\circ$  latitude bands. This approach assumed that the stations on which the MLR analyses were performed adequately represented the zonal variations in depth-integrated  $\delta^{13}\text{C}$  values. This assumption was evaluated by using the depth-integrated  $\delta^{13}\text{C}$  changes at 27 stations on cruise P06 which was an east-west cruise along  $32^\circ\text{S}$  that extended zonally across the entire basin. Including these 27 stations with 7 additional stations sampled during the north-south cruises P18 and P16S in the same latitude band ( $30^\circ\text{S}$ – $40^\circ\text{S}$ ) yielded a mean depth-integrated  $\delta^{13}\text{C}$  change rate of  $-127 \pm 8\text{‰ m decade}^{-1}$ , whereas relying only on the 7 stations on P18 and P16S cruises yielded  $-103 \pm 24\text{‰ m decade}^{-1}$ . In this latitude band an underestimate of  $\sim 20 \pm 20\%$  for the zonal mean would occur by relying only on north-south cruises. To broaden the test of spatial bias a similar analysis of  $\delta^{13}\text{C}$  changes predicted by Modular Ocean Model (MOM) was used. The sampling bias ranged from  $-12$  to  $+30\%$  and was well within the uncertainty of the observed depth-integrated  $\delta^{13}\text{C}$  change in 12 of 13 latitude bands. The bias on a basin-wide scale was  $< 1\%$  (i.e., regional biases were offsetting) and small compared to an uncertainty of  $\pm 20\%$  in the mean  $\delta^{13}\text{C}$  inventory change. The MOM output indicated that spatial biases in the data set likely did not significantly impact either the latitudinal trend of observed depth-integrated  $\delta^{13}\text{C}$  change or the basin-wide average.

Temporal biases in the surface ocean  $\delta^{13}\text{C}$  change resulting from seasonal differences in sampling times between the cruises in 1990s and 2000s were evaluated. The monthly distribution of surface  $\delta^{13}\text{C}$  data from the 1990s and 2000s was determined over  $10^\circ$  latitude bands. To test for seasonal biases the mean  $\delta^{13}\text{C}$  difference between decades was determined by using the monthly distribution  $\delta^{13}\text{C}$  values in the 1990s to weight the monthly data distribution in the 2000s and then compared to the  $\delta^{13}\text{C}$  difference without any weighting. The  $\delta^{13}\text{C}$  difference between these two approaches was not significant ( $< 0.04\text{‰}$ ) within  $30^\circ$  of the equator but was significant at  $-0.23$  to  $0.14\text{‰}$  poleward of  $30^\circ$ . The monthly weighting approach was used to determine surface ocean  $\delta^{13}\text{C}$  changes.

The estimated DIC inventory change at each station was determined by multiplying the depth-integrated  $\delta^{13}\text{C}$  change by the mean RC determined for each cruise. Thus, the error in the DIC inventory change was a result of the errors in the  $\delta^{13}\text{C}$  inventory change and RC which yielded typical errors of 20–30%.

The error in the air-sea  $\delta^{13}\text{C}$  disequilibrium was determined following the procedure used by Quay *et al.* [2007] which combined the errors in the measured  $\delta^{13}\text{C}$  of the surface ocean DIC and the fractionation

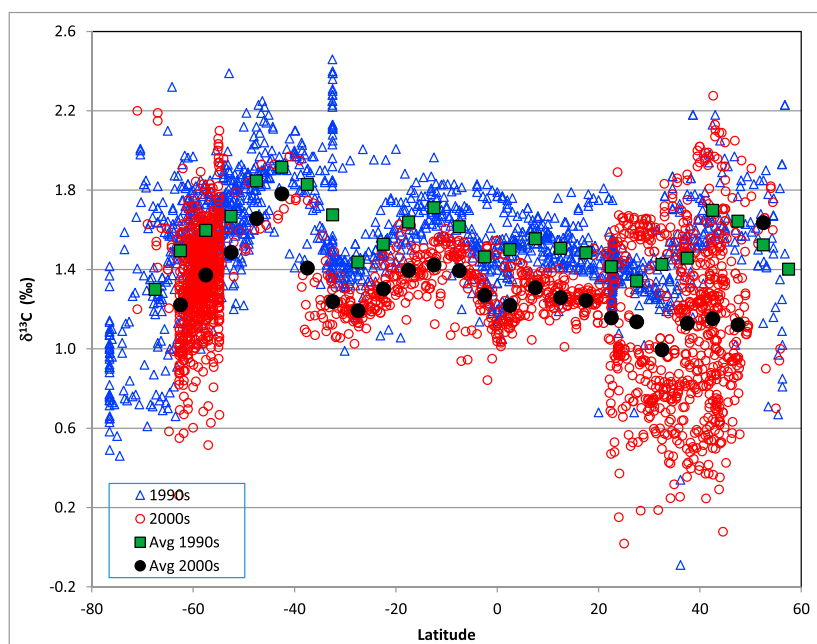


**Figure 2.** Spatial trends of measured  $\delta^{13}\text{C}$  (‰) during the 1990s and 2000s ( $n = 3457$ ) in surface layer of Pacific Ocean. Solid symbols represent mean value over  $5^\circ$  latitude band.

factor between DIC and  $\text{CO}_2$  gas, i.e.,  $\pm 0.1\text{‰}$  [Zhang *et al.*, 1995]. The standard error (SE) in the mean  $\delta^{13}\text{C}$  for a given latitude band was assumed to equal  $2 * \text{SD} / \sqrt{(N - 1)}$  where  $N$  equaled the number of observations. The SE of the  $\delta^{13}\text{C}$  disequilibrium averaged over  $5^\circ$  latitude bands ranged from  $\pm 0.04\text{‰}$  in the equatorial region to  $\pm 0.19\text{‰}$  north of  $50^\circ\text{N}$  where seasonality in  $\delta^{13}\text{C}$  was higher and averaged  $\pm 0.07\text{‰}$  for the basin.

The anthropogenic  $\text{CO}_2$  uptake rate was estimated over  $10^\circ$  latitude intervals from the difference between the mean  $\text{DIC}^{13}$  inventory change and gross air-sea  $^{13}\text{CO}_2$  flux over each interval with the error in the uptake estimate depending on the combined errors in the  $\text{DIC}^{13}$  inventory change and  $^{13}\text{CO}_2$  flux.

Uncertainties in the mean RC value for each cruise represented the variability ( $\pm 1$  SD) of RC values calculated from  $\delta^{13}\text{C}$  and DIC residuals determined by the eMLR method for each isopycnal surface analyzed. At the HOT and Drake Passage time series sites, the error in RC depended on the SEs of the linear regressions of MLR-based  $\delta^{13}\text{C}$  and DIC residuals versus time.

#### 2.4. Ocean Model

The results from the  $\delta^{13}\text{C}$  observations were compared to model-based estimates of the anthropogenic  $\text{CO}_2$  and  $\delta^{13}\text{C}$  changes in the ocean. A version of the Modular Ocean Model (MOM-3 P2A [Gnanadesikan *et al.*, 2004]) was used with zonal and meridional grid resolutions of  $4^\circ \times 4.5^\circ$ , 24 vertical levels including a Gent-McWilliams along-isopycnal mixing scheme [Gent and McWilliams, 1990] and driven by steady climatological winds that varied seasonally. The model's application to the anthropogenic  $\text{CO}_2$  and  $\delta^{13}\text{C}$  perturbation was fully described in Sonnerup and Quay [2012]. Briefly,  $^{13}\text{C}$  was added to the Ocean Carbon-Cycle Model Intercomparison Project (OCMIP) geochemical cycling scheme, using equilibrium and kinetic isotope  $\text{CO}_2$  fractionations from Zhang *et al.* [1995]. The model's  $^{13}\text{CO}_2$  and  $^{12}\text{CO}_2$  fields were equilibrated (15,000 model years) with the preindustrial atmosphere with  $\text{pCO}_2$  of 278 ppm and  $\delta^{13}\text{C}$  of  $-6.3\text{‰}$  [Francey *et al.*, 1999]. The model was then forced with the OCMIP atmospheric  $\text{pCO}_2$  and  $\delta^{13}\text{C}$  time histories from ice cores augmented with measurements of  $\text{pCO}_2$  at Mauna Loa and  $\delta^{13}\text{C}$  at Cape Grim [Francey *et al.*, 1999; Orr, 2002]. The model neglected riverine input of organic carbon which is on the order of  $0.4 \text{ Gt C yr}^{-1}$  [Sarmiento and Sundquist, 1992; Siegenthaler and Sarmiento, 1993] and would deplete the preindustrial ocean's  $\delta^{13}\text{C}$  by  $\sim 0.1\text{‰}$  so this  $\delta^{13}\text{C}$  offset was applied to the model  $\delta^{13}\text{C}$  output when needed for comparisons to  $\delta^{13}\text{C}$  observations. This model will be referred to as MOM when reporting results.

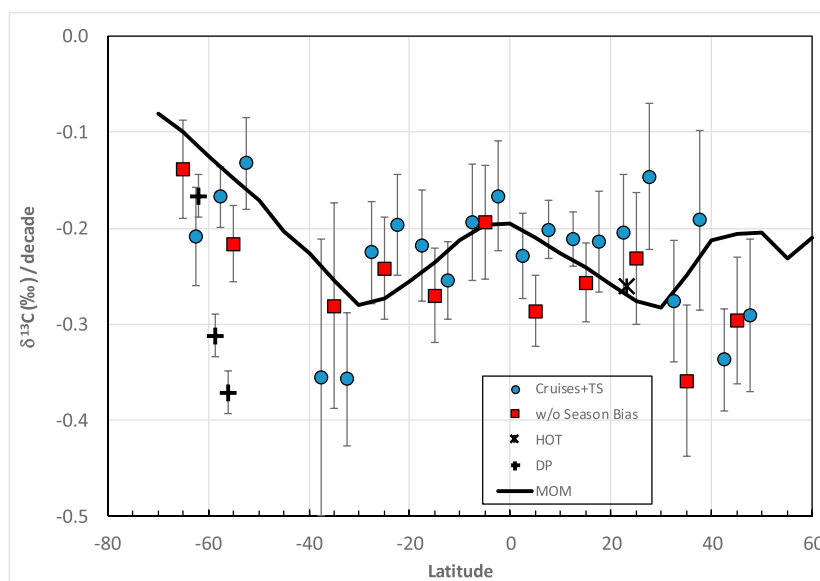


**Figure 3.**  $\delta^{13}\text{C}$  change rate ( $\text{‰ decade}^{-1}$ ) of surface layer of Pacific Ocean (mean and SD of data binned into latitude bands) based on measurements during the 1990s and 2000s and corrected for seasonal sampling biases, see text, and on time series  $\delta^{13}\text{C}$  measurements at HOT (23°N, 158°W) and Drake Passage (55°S–63°S, ~63°W), with the latter sorted by latitude. Surface  $\delta^{13}\text{C}$  change rate from MOM simulation is shown.

### 3. Results and Discussion

#### 3.1. Surface Ocean $\delta^{13}\text{C}$ Change

Although the meridional trend in  $\delta^{13}\text{C}$  in the surface ocean of the Pacific was well preserved between the 1990s and 2000s ( $n = 3457$ ) there was a clear decrease (Figure 2). The  $\delta^{13}\text{C}$  variability increased significantly between the 1990s and 2000s primarily in two regions (55°S–65°S and 20°N–50°N). This was a result of adding  $\delta^{13}\text{C}$  measurements from a time series in the Drake Passage (2005–2015) and from 18 container ship cruises across the North Pacific (2008–2015). In both cases, sampling occurred year round and thus expanded the seasonal coverage of the  $\delta^{13}\text{C}$  data set as compared with research cruises in the 1990s which mainly occurred in summer. To account for possible seasonal bias in sampling times the surface  $\delta^{13}\text{C}$  change was determined by using the same monthly distribution of sampling times in both data sets from the 1990s and 2000s, as described above. The surface  $\delta^{13}\text{C}$  time rate of change (seasonal bias corrected) varied from  $\sim -0.15$  to  $-0.35\text{‰ decade}^{-1}$  averaged over  $10^\circ$  latitude bands (Figure 3) and yielded a basin-wide mean of  $-0.20 \pm 0.06\text{‰ decade}^{-1}$  that was similar to the previous estimate of  $-0.18 \pm 0.06\text{‰ decade}^{-1}$  observed between the 1970s and 1990s [Quay *et al.*, 2003]. MOM predicted a basin-wide surface ocean  $\delta^{13}\text{C}$  decrease of  $-0.23\text{‰ decade}^{-1}$  in the 1990s that agreed well with the observed mean change and a meridional trend of surface  $\delta^{13}\text{C}$  change that agreed with observations equatorward of  $40^\circ$  but underestimated the observed change poleward of  $40^\circ$  (Figure 3).

Decade-long time series of the surface ocean  $\delta^{13}\text{C}$  and DIC changes were measured at a subtropical site in the North Pacific (HOT) and Southern Ocean site (Drake Passage or DP) (Figure 4). At both sites the MLR method was used to determine the anthropogenic  $\delta^{13}\text{C}$  and DIC time rate of change by accounting for the temporal changes that were the result of changes in temperature, salinity, and phosphate. At HOT in the subtropical North Pacific surface ocean  $\delta^{13}\text{C}$  measured between 1991 and 2012 ( $n = 516$ ) yielded a decrease rate of  $-0.25 \pm 0.01\text{‰ decade}^{-1}$  and a DIC increase of  $14 \pm 1 \mu\text{mol kg}^{-1} \text{ decade}^{-1}$ . The  $\delta^{13}\text{C}$  decrease at HOT was similar to the rate determined from cruise data in this region (20°N–30°N) at  $-0.23 \pm 0.07\text{‰ decade}^{-1}$  and the  $-0.24\text{‰ decade}^{-1}$  rate observed at the Bermuda Time Series station in the subtropical North Atlantic [Gruber *et al.*, 2002]. For comparison, a surface ocean in equilibrium with the atmosphere would yield a  $\delta^{13}\text{C}$  decrease of  $\sim -0.27\text{‰ decade}^{-1}$  between the 1990s and 2000s.

The Drake Passage (DP) surface ocean  $\delta^{13}\text{C}$  time series measurements between 2005 and 2014 yielded rates of anthropogenic  $\delta^{13}\text{C}$  decrease at  $-0.28 \pm 0.02\text{‰ decade}^{-1}$  (Figure 4) and DIC increase at

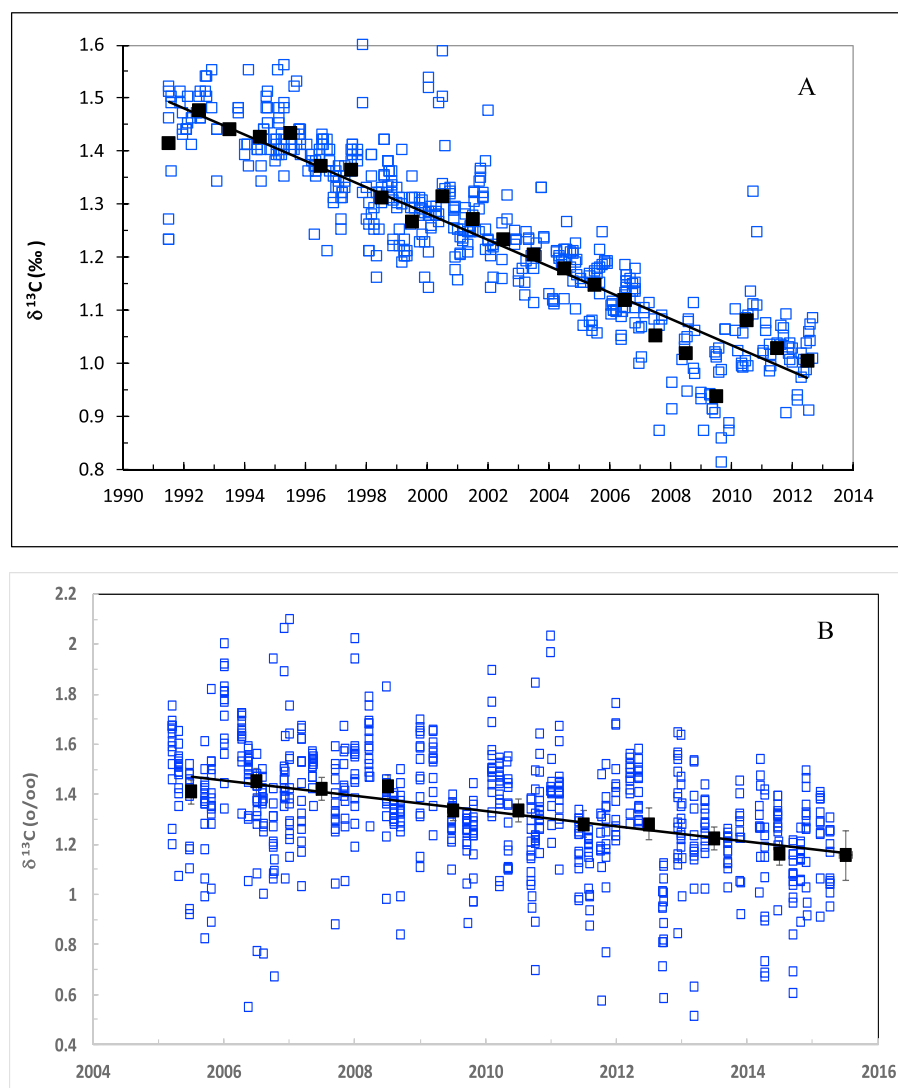


**Figure 4.** The  $\delta^{13}\text{C}$  time histories in the surface layer at (a) the Hawaii Ocean Time Series site (HOT) in the subtropical North Pacific Ocean ( $23^\circ\text{N}$ ,  $158^\circ\text{W}$ ) over the last 20 years and at (b) the Drake Passage time series site ( $55^\circ\text{S}$ – $63^\circ\text{S}$  and  $68^\circ\text{W}$ – $58^\circ\text{W}$ ). Annual means represented by solid squares.

$14 \pm 2 \mu\text{mol kg}^{-1} \text{decade}^{-1}$ . Sorting the DP time series data by latitude the  $\delta^{13}\text{C}$  and DIC changes were  $-0.37 \pm 0.05$ ,  $-0.30 \pm 0.04$ , and  $-0.19 \pm 0.05\text{‰ decade}^{-1}$  and  $20 \pm 6$ ,  $14 \pm 3$ , and  $8 \pm 4 \mu\text{mol kg}^{-1} \text{decade}^{-1}$  for  $55^\circ\text{S}$ – $57^\circ\text{S}$ ,  $57^\circ\text{S}$ – $60^\circ\text{S}$ , and  $60^\circ\text{S}$ – $63^\circ\text{S}$ , respectively. The magnitude of the  $\delta^{13}\text{C}$  change at DP was significantly greater than indicated by cruise data ( $-0.19 \pm 0.04\text{‰ decade}^{-1}$ ) or MOM output ( $-0.12\text{‰ decade}^{-1}$ ) at these latitudes although the observed poleward decrease was expected (Figure 3).

The DIC and  $\delta^{13}\text{C}$  changes between  $55^\circ\text{S}$  and  $60^\circ\text{S}$  were significantly higher than the changes of  $8 \mu\text{mol kg}^{-1} \text{decade}^{-1}$  and  $-0.22\text{‰ decade}^{-1}$  expected if the surface ocean maintained equilibrium with atmospheric  $\text{pCO}_2$  and  $\delta^{13}\text{C}$  between 2005 and 2015 imply higher than average anthropogenic  $\text{CO}_2$  accumulation in the DP region. A high rate of anthropogenic  $\text{CO}_2$  accumulation at DP appears to support the observations of Landschützer *et al.* [2015] who concluded that anthropogenic  $\text{CO}_2$  uptake in the Southern Ocean has been accelerating since 2002 based on their analysis of surface ocean  $\text{pCO}_2$  data and an inversion of atmospheric  $\text{CO}_2$  data. Landschützer *et al.* attributed the accelerated  $\text{CO}_2$  uptake in the Pacific sector of the South Ocean mainly to cooling of surface waters rather than a decrease in upwelling rate. Although cooling would enhance surface ocean uptake of  $\text{CO}_2$  it would reduce the  $\delta^{13}\text{C}$  decrease rate because of the temperature dependence of the  $\delta^{13}\text{C}$  fractionation effect between DIC and  $\text{CO}_2$  gas [Zhang *et al.*, 1995]

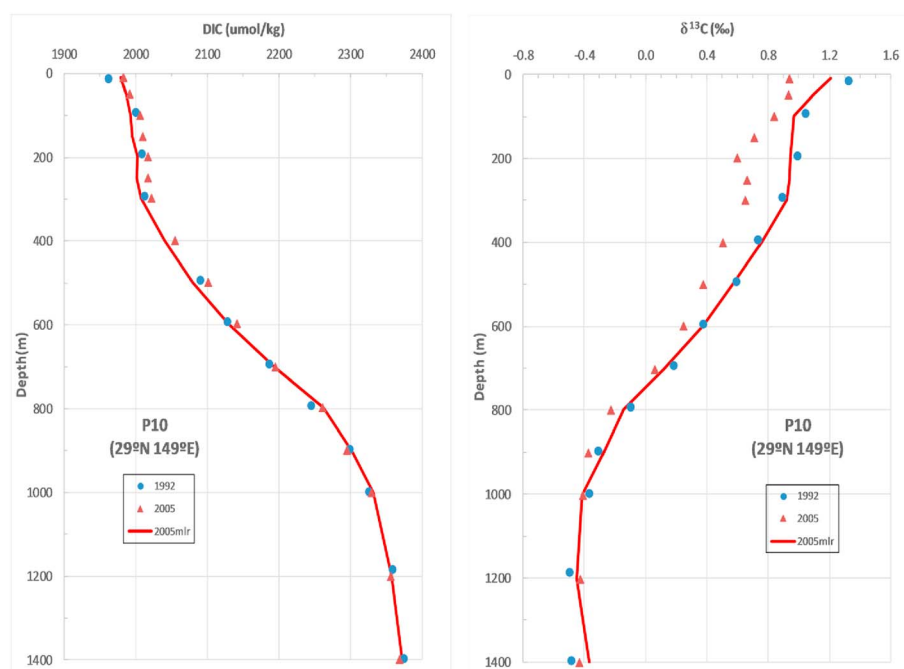


**Figure 5.**  $\delta^{13}\text{C}$  and DIC depth profiles measured on cruise P10 in 1992 and 2005 at a location of  $29^\circ\text{N}$  and  $149^\circ\text{E}$ . The MLR prediction of the  $\delta^{13}\text{C}$  and DIC depth profiles in 2005 is shown. The difference between measured and predicted  $\delta^{13}\text{C}$  and DIC values in 2005 is assumed to represent anthropogenic change.

which in turn would increase the air-sea  $\delta^{13}\text{C}$  disequilibrium, discussed below. Thus, the higher than expected  $\delta^{13}\text{C}$  decrease rate at DP is at odds with surface cooling being the sole mechanism for increasing anthropogenic  $\text{CO}_2$  uptake at this site.

### 3.2. Depth Distribution of Anthropogenic $\delta^{13}\text{C}$ Change

Changes in the depth distribution of anthropogenic  $\delta^{13}\text{C}$  change were determined at  $\sim 127$  stations where  $\delta^{13}\text{C}$  depth profiles were measured at the same location during WOCE and CLIVAR programs. Typically, direct comparison of the measured  $\delta^{13}\text{C}$  depth profiles at a station showed a clear  $\delta^{13}\text{C}$  decrease between the 1990s and 2000s with the greatest  $\delta^{13}\text{C}$  change occurring at the surface ( $\sim -0.2$  to  $-0.4\text{‰}$ ) and decreasing with depth to a maximum of  $\sim 1000$  m (Figure 5). The anthropogenic component of the measured  $\delta^{13}\text{C}$  depth change was represented by the difference between the recently measured  $\delta^{13}\text{C}$  depth profile and the MLR-predicted depth profile at that time. Usually the depth trend in anthropogenic  $\delta^{13}\text{C}$  change determined by the MLR approach was similar in magnitude to the directly measured  $\delta^{13}\text{C}$  change and had a stronger signal than the anthropogenic DIC change, i.e., the eMLR-derived  $\delta^{13}\text{C}$  and DIC changes were  $\sim 4\times$  and  $2\times$  the eMLR uncertainties, respectively (Figure 5).

The eMLR method was used to estimate depth-integrated anthropogenic  $\delta^{13}\text{C}$  change at each station (Table S1). A minimum significant  $\delta^{13}\text{C}$  residual (typically  $\sim 0.1\text{‰}$ ) was selected based on the error in the eMLR fits to the  $\delta^{13}\text{C}$  data sets for each cruise (Table S2), and the depth profile of  $\delta^{13}\text{C}$  change was integrated downward to the depth where the minimum  $\delta^{13}\text{C}$  residual was reached. The  $\delta^{13}\text{C}$  change results of an eMLR-based depth-integrated  $\delta^{13}\text{C}$  change (predicted-predicted) were similar to a MLR-based  $\delta^{13}\text{C}$  change (measured-predicted) at the 127 stations examined; i.e., on a basin-wide scale the two approaches agreed within 3%. The error in the depth-integrated  $\delta^{13}\text{C}$  change at individual stations was typically  $\sim \pm 10\text{--}20\%$  (Table S1).

A meridional cross section of the estimated anthropogenic  $\delta^{13}\text{C}$  change showed the largest and deepest change occurred between  $30^\circ\text{S}$  and  $55^\circ\text{S}$ , whereas the smallest and shallowest change occurred in the Southern Ocean (south of  $60^\circ\text{S}$ ) and subpolar North Pacific (north of  $50^\circ\text{N}$ ) (Figure 6). The anthropogenic  $\delta^{13}\text{C}$  change was larger and extended deeper in the subtropics ( $20\text{--}40^\circ$ ) than in the equatorial ( $15^\circ\text{S}\text{--}15^\circ\text{N}$ )

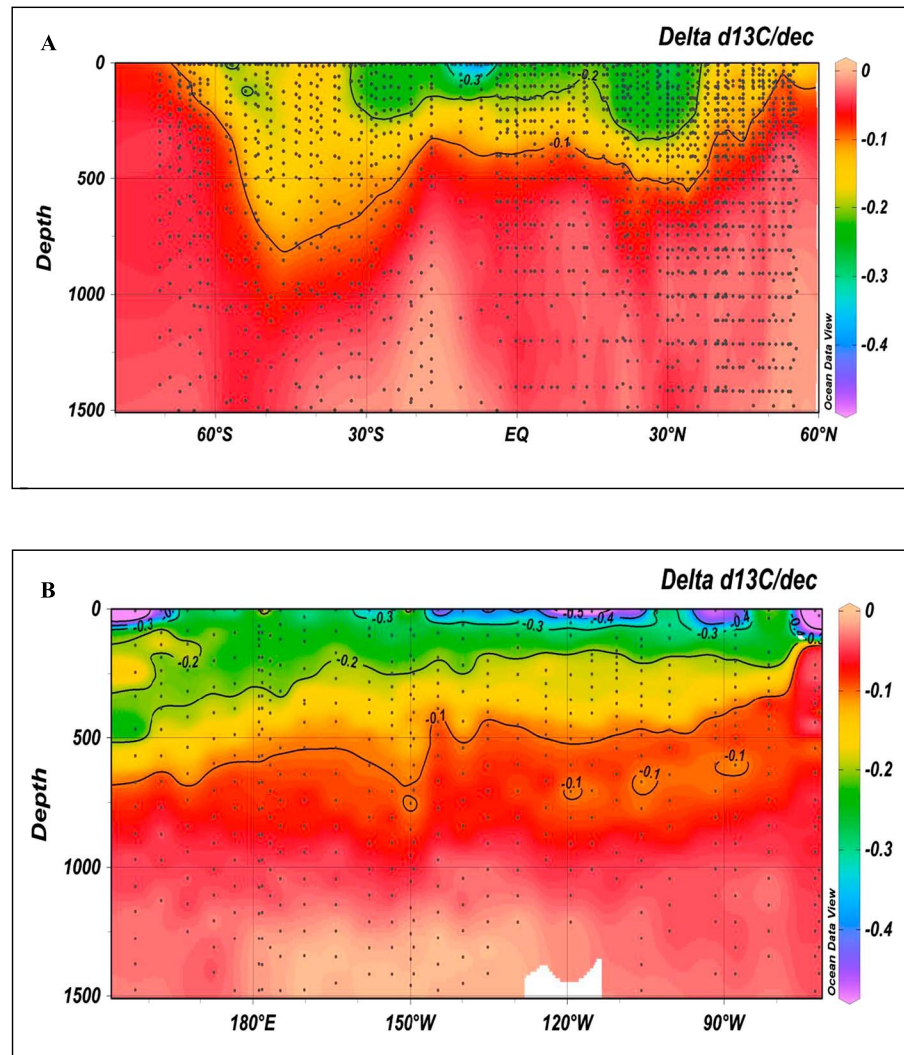


**Figure 6.** (a) Meridional and (b) zonal cross sections of the anthropogenic  $\delta^{13}\text{C}$  change (‰ decade<sup>-1</sup>) in the Pacific Ocean based on results of the eMLR method. The meridional cross section represents a compilation of five cruises (P10, P16S, P16N, P17, and P18), and the zonal cross section represents results from cruise P06 which is an east-west cruise along 32°S.

region. These trends in anthropogenic  $\delta^{13}\text{C}$  change were similar to those observed in the Indian Ocean [Sonnerup *et al.*, 2000] and along P18 in the South Pacific (one of the cruises analyzed here) [Ko *et al.*, 2014]; both these studies showed a clear correlation between the anthropogenic  $\delta^{13}\text{C}$  change and CFC tracer concentration. The zonal cross section of the anthropogenic  $\delta^{13}\text{C}$  change at 32°S showed a deeper penetration in the western portion of the basin than eastern portion (Figure 6) a trend similar to that observed for anthropogenic DIC change estimated by Waters *et al.* [2011].

### 3.2.1. Latitudinal Trends in Anthropogenic $\delta^{13}\text{C}$ Change

There was a clear latitudinal trend in magnitude of the depth-integrated  $\delta^{13}\text{C}$  change (Figure 7). The greatest  $\delta^{13}\text{C}$  change occurred between 30°S and 60°S at  $-129 \pm 27$ ‰ m decade<sup>-1</sup>, which was twofold greater than in the equatorial Pacific (15°S to 15°N) at  $-63 \pm 17$ ‰ m decade<sup>-1</sup>. The smallest  $\delta^{13}\text{C}$  change occurred in the Southern Ocean (south of 60°S) and in the subpolar North Pacific (north of 50°N) at  $-20$  to  $-30$ ‰ m decade<sup>-1</sup>. It is worth noting that the highest depth-integrated  $\delta^{13}\text{C}$  change rate was observed between 50°S and 60°S along 105°W (P18) which is within the footprint of the DP time series which showed anomalously high surface anthropogenic  $\delta^{13}\text{C}$  change. Both observations suggest that this region may be a site of high anthropogenic CO<sub>2</sub> accumulation.

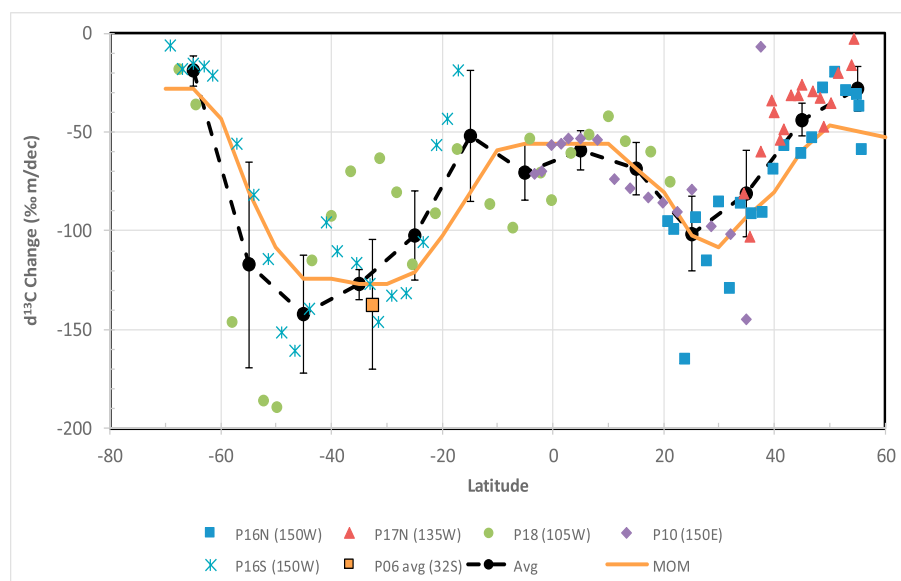


**Figure 7.** The latitudinal trends in the depth-integrated anthropogenic  $\delta^{13}\text{C}$  change ( $\text{‰ m decade}^{-1}$ ) in the Pacific Ocean determined by using the eMLR approach at 127 stations pairs with mean values ( $\pm\text{SE}$  in mean) over  $10^\circ$  latitude intervals (dashed line) and predicted by (zonally averaged) MOM (solid line).

The observed latitudinal trend and magnitude of the depth-integrated  $\delta^{13}\text{C}$  change agreed with previous observations. *Quay et al.* [2003] estimated a range from 0 to  $-90\text{‰ m decade}^{-1}$  for the Pacific Ocean between the 1970s and 1990s with smaller changes in the equatorial and subpolar North Pacific than the subtropical ocean. *Sonnerup et al.* [2000] estimated integrated  $\delta^{13}\text{C}$  change that ranged from 0 to  $-122\text{‰ m decade}^{-1}$  for the Indian Ocean between the 1970s and 1990s with minimal change in the equatorial region and maximum change between  $25^\circ\text{S}$  to  $40^\circ\text{S}$ . *Ko et al.* [2014] found similar magnitude and latitudinal dependence for the integrated  $\delta^{13}\text{C}$  change between the 1990s and 2000s along P18 that ranged from a maximum of  $\sim -150 \pm 10\text{‰ m decade}^{-1}$  between  $35^\circ\text{S}$  and  $55^\circ\text{S}$  to a minimum of  $\sim -50\text{‰ m decade}^{-1}$  in the Southern Ocean and equatorial Pacific. In contrast, there was only a slight longitudinal trend in depth-integrated  $\delta^{13}\text{C}$  change across the basin along  $32^\circ\text{S}$  (i.e., the mean values were  $-137 \pm 7$  and  $-129 \pm 10\text{‰ m decade}^{-1}$  in the western and eastern halves of the basin, respectively). The mean-integrated  $\delta^{13}\text{C}$  change for the South Pacific at  $-96 \pm 25\text{‰ m decade}^{-1}$  was about 50% higher than in the North Pacific at  $-68 \pm 15\text{‰ m decade}^{-1}$  and yielded a basin-wide mean of  $-83 \pm 20\text{‰ m decade}^{-1}$ . The mean  $\delta^{13}\text{C}$  change for the Pacific Ocean was similar to the  $-69 \pm 5\text{‰ m decade}^{-1}$  estimated by *Sonnerup et al.* [2000] for the Indian Ocean between the 1970s and 1990s, but only about half the  $-150 \pm 38\text{‰ m decade}^{-1}$  for the North Atlantic Ocean between the 1990s and 2000s [*Quay et al.*, 2007].

The penetration depth of the  $\delta^{13}\text{C}$  change ranged from  $\sim 100$  to  $1100$  m for individual stations and showed the same latitudinal trend as the integrated  $\delta^{13}\text{C}$  change with deepest penetration occurring between  $30^\circ\text{S}$  to  $50^\circ\text{S}$  (mean =  $\sim 900$  m) and the shallowest penetration occurring north of  $50^\circ\text{N}$  and south of  $60^\circ\text{S}$  (mean =  $\sim 150$  m). The basin-wide mean penetration depth of  $\sim 480$  m was  $\sim 20\%$  greater than the global mean penetration depth of  $405$  m estimated between the 1970s and 1990s [*Quay et al.*, 2003]. In contrast, a mean penetration depth of the anthropogenic  $\delta^{13}\text{C}$  change in the North Atlantic was  $\sim 3$ -fold greater at  $\sim 1500$  m [*Quay et al.*, 2007].

The MOM-predicted depth-integrated  $\delta^{13}\text{C}$  change with a mean basin change of  $-83\text{‰ m decade}^{-1}$  agreed well with the observed change ( $-83 \pm 20\text{‰ m decade}^{-1}$ ) as does the meridional trend (Figure 7). The agreement between MOM predictions and observed depth-integrated  $\delta^{13}\text{C}$  changes in the Pacific Ocean indicates that the model generally achieved an accurate balance of air-sea exchange and ventilation of thermocline waters needed to reproduce the observed anthropogenic  $\delta^{13}\text{C}$  changes. These results support the expectation that because this MOM configuration yielded representative CFC fields in the ocean [*Matsumoto et al.*, 2004], it should yield representative anthropogenic  $\delta^{13}\text{C}$  and  $\text{CO}_2$  changes in the ocean.

### 3.2.2. DIC<sup>13</sup> Inventory Change

The DIC<sup>13</sup> inventory change ( $\text{‰ mol m}^{-2} \text{decade}^{-1}$ ) was composed of two components, i.e., the  $\delta^{13}\text{C}$  change multiplied by the mean DIC concentration and the DIC change multiplied by the mean  $\delta^{13}\text{C}$  over the integration range (i.e.,  $\Delta\text{DIC}^{13} = \text{DIC}_r(\delta^{13}\text{C}_r - \delta^{13}\text{C}_p) + \delta^{13}\text{C}_p(\text{DIC}_r - \text{DIC}_p)$ , where  $p$  is previous and  $r$  is recent). The DIC<sup>13</sup> change was dominated by the first term. For example, the mean basin-wide average value of  $\text{DIC}_r \cdot \Delta\delta^{13}\text{C}$  was  $-178 \pm 43 \text{‰ mol m}^{-2} \text{decade}^{-1}$ , whereas the value of  $\delta^{13}\text{C}_p \cdot \Delta\text{DIC}$  was  $5 \text{‰ mol m}^{-2} \text{decade}^{-1}$ .

The DIC<sup>13</sup> inventory change rate was compared to the air-sea <sup>13</sup>CO<sub>2</sub> flux rate, as discussed below. In a 1-D vertical ocean (with no external input or loss) these two rates should be equal and an imbalance between these rates on regional scales can be used to estimate horizontal transport of the anthropogenic  $\delta^{13}\text{C}$  signal. The latitudinal trend in integrated DIC<sup>13</sup> change followed the latitudinal trend in the  $\delta^{13}\text{C}$ -integrated change because the mean DIC concentration over the integration depth ( $\sim 2150 \mu\text{mol kg}^{-1}$ ) showed little spatial variation.

### 3.3. Anthropogenic CO<sub>2</sub> Inventory Change

The anthropogenic CO<sub>2</sub> (DIC) inventory change between the 1990s and 2000s was estimated from the depth-integrated  $\delta^{13}\text{C}$  change. The approach required an estimate of the ratio of anthropogenic  $\delta^{13}\text{C}/\text{CO}_2$  change (RC), as described above. The CO<sub>2</sub> inventory changes at each station was computed from the depth-integrated  $\delta^{13}\text{C}$  change divided by RC. RC values were estimated from the ratio of the eMLR-based  $\delta^{13}\text{C}$  and DIC residuals on each isopycnal surface from which a mean value of RC was estimated for the entire cruise and yielded values of  $-0.020 \pm 0.002$ ,  $-0.025 \pm 0.008$ ,  $-0.022 \pm 0.004$ ,  $-0.026 \pm 0.010$ ,  $-0.018 \pm 0.002$ , and  $-0.016 \pm 0.002 \text{‰} (\mu\text{mol kg}^{-1})^{-1}$  respectively, for P06, P10, P16S, P16N, P17, and P18. At HOT, the surface ocean  $\delta^{13}\text{C}$  decrease (Figure 4) and DIC increase over the last 20 years yielded a direct estimate of  $\text{RC} = -0.018 \pm 0.002 \text{‰} (\mu\text{mol kg}^{-1})^{-1}$ . RC estimates have been shown to change significantly in the Southern Ocean and is likely related to reduced surface water exposure times [McNeil *et al.*, 2001]. A mean value of  $\text{RC} = -0.010 \pm 0.002 \text{‰} (\mu\text{mol kg}^{-1})^{-1}$  was determined at stations south of 60°S ( $n=4$ ) on P16S and P18, which agrees well with previous estimates in the Southern Ocean [Sonnerup and Quay, 2012], and this RC value was used to estimate anthropogenic CO<sub>2</sub> change for stations south of 60°S on these cruises. The DP time series site, which showed anomalously high rates of surface anthropogenic  $\delta^{13}\text{C}$  and DIC change, showed anomalously low (more negative) surface ocean RC value of  $-0.021 \pm 0.003 \text{‰} (\mu\text{mol kg}^{-1})^{-1}$  when compared to RC estimates along isopycnals at these latitudes.

The estimated anthropogenic CO<sub>2</sub> inventory change (Figure 8) ranged from 0.1 to 0.7 mol C m<sup>-2</sup> yr<sup>-1</sup> with a meridional trend that followed the trend for depth-integrated  $\delta^{13}\text{C}$  change (Figure 7). The highest CO<sub>2</sub> inventory changes occurred between 30°S and 60°S and lowest occurred in the subpolar North Pacific and Southern Ocean and yielded a mean basin-wide rate of  $0.41 \pm 0.13 \text{ mol m}^{-2} \text{ yr}^{-1}$  ( $0.82 \pm 0.26 \text{ Pg yr}^{-1}$ ). Possible biases in these estimates resulting from cruise track locations were expected to be within the reported uncertainties of the estimated regional anthropogenic CO<sub>2</sub> inventory change, as discussed above.

The  $\delta^{13}\text{C}$ -based anthropogenic CO<sub>2</sub> inventory changes agreed well (within  $\pm 10\%$ ) with previous estimates of anthropogenic CO<sub>2</sub> change for the Pacific Ocean (Figure 8 and Table 2). This agreement was not surprising as several of the previous estimates utilized a MLR approach to estimate anthropogenic CO<sub>2</sub> change on some of the same cruises on which MLR approach was used here to determine RC. Sabine *et al.*'s [2008] MLR-based estimate of anthropogenic CO<sub>2</sub> change on P16 (70°S to 60°N along 150°W) yielded a clear picture of the meridional trend in CO<sub>2</sub> inventory change that agreed well with the  $\delta^{13}\text{C}$ -based estimates (Figure 8); the two trends were independent of each other because a single value of RC was used to convert  $\delta^{13}\text{C}$  to CO<sub>2</sub> inventory change for the entire P16 cruise. The  $\delta^{13}\text{C}$ -based estimates of anthropogenic CO<sub>2</sub> inventory change for the South and North Pacific at  $0.51 \pm 0.17$  and  $0.31 \pm 0.09 \text{ mol m}^{-2} \text{ yr}^{-1}$ , respectively, and basin-wide mean of  $0.41 \pm 0.13 \text{ mol m}^{-2} \text{ yr}^{-1}$  ( $0.82 \pm 0.26 \text{ Pg yr}^{-1}$ ) were comparable to Sabine *et al.*'s [2008] estimates of 0.41, 0.25 and 0.33 mol m<sup>-2</sup> yr<sup>-1</sup>, respectively. The  $\delta^{13}\text{C}$ -based anthropogenic CO<sub>2</sub> inventory change rate on east-west cruise P06 along 32°S yielded an estimate of  $0.66 \pm 0.15 \text{ mol m}^{-2} \text{ yr}^{-1}$  for the eastern half of the basin (east of 170°W) that was indistinguishable from the uptake rate in the western half at  $0.71 \pm 0.20 \text{ mol m}^{-2} \text{ yr}^{-1}$ . This trend contrasts with Waters *et al.*'s [2011] conclusion that the CO<sub>2</sub> uptake rate in the eastern portion (at  $0.87 \pm 0.1 \text{ mol m}^{-2} \text{ yr}^{-1}$ ) exceeded

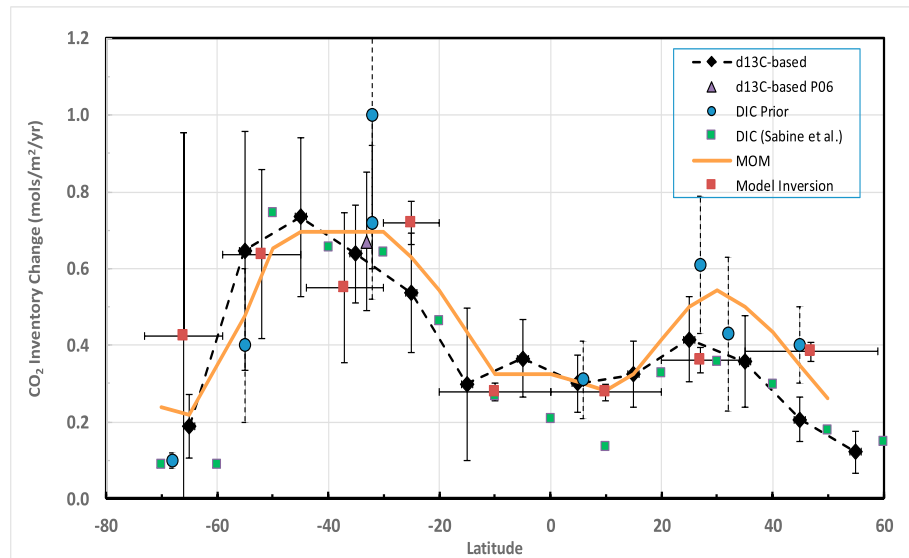


**Figure 8.** The anthropogenic CO<sub>2</sub> inventory change ( $\text{mol C m}^{-2} \text{yr}^{-1}$ ) estimated from compiled depth-integrated  $\delta^{13}\text{C}$  inventory changes along P10, P16, P17, and P18 (dashed line) and zonal mean for P06. Also shown are anthropogenic CO<sub>2</sub> changes estimated previously for the Pacific Ocean (see Table 2) including the latitudinal trend for P16 (along  $\sim 150^\circ\text{W}$ ) reported by Sabine et al. [2008] and zonally averaged estimates from MOM (solid line) and previous model inversion [Gruber et al., 2009].

the western portion (at  $0.66 \pm 0.1 \text{ mol m}^{-2} \text{yr}^{-1}$ ) of the cruise track by  $\sim 30\%$ . In the two instances where disagreement with previous results exceeded  $\pm 10\%$  (Table 2) a non-MLR approach had been used to estimate anthropogenic CO<sub>2</sub> change [Murata et al., 2007, 2009].

MOM-predicted anthropogenic CO<sub>2</sub> inventory changes agreed well with the  $\delta^{13}\text{C}$ -based estimates (Figure 8) and had a similar range ( $0.2$  to  $0.7 \text{ mol m}^{-2} \text{yr}^{-1}$ ) and mean basin-wide value of  $0.46 \text{ mol m}^{-2} \text{yr}^{-1}$  ( $0.92 \text{ Pg yr}^{-1}$ ). The model's meridional trend in CO<sub>2</sub> inventory change matched the  $\delta^{13}\text{C}$ -based trend with lowest inventory changes in the Southern Ocean and subpolar North Pacific and greatest change in the S. Pacific between  $30^\circ\text{S}$  and  $50^\circ\text{S}$ . Khatiwala et al. [2013] used a chlorofluorocarbon (CFC)-tuned transit time distribution method to estimate anthropogenic CO<sub>2</sub> inventory change rate of  $0.46 \pm 0.09 \text{ mol m}^{-2} \text{yr}^{-1}$  for the Pacific Ocean in 1998 (the mean collection year for the  $\delta^{13}\text{C}$  data in this study) that agreed well with the  $\delta^{13}\text{C}$ -based estimate. Gruber et al.'s [2009] estimated an anthropogenic CO<sub>2</sub> inventory change rate in the 1990s of  $0.42 \pm 0.07 \text{ mol m}^{-2} \text{yr}^{-1}$  ( $\sim 0.83 \pm 0.13 \text{ Pg yr}^{-1}$ ) for the Pacific Ocean (north of  $58^\circ\text{S}$ ) based on

**Table 2.** Anthropogenic CO<sub>2</sub> Accumulation Rates in the Pacific Ocean Between the 1990s and 2000s Based on DIC and  $\delta^{13}\text{C}$  Observations and Predicted by MOM

Region (Cruise)	Method	Accumulation Rate ( $\text{mol m}^{-2} \text{yr}^{-1}$ )	Reference
67°S (S04P)	eMLR	$0.10 \pm 0.02$	Williams et al. [2015]
32°S (P06)	eMLR	$0.7 \pm 0.2$	Waters et al. [2011]
32°N (P02)	eMLR	$0.43 \pm 0.1$	Sabine et al. [2008]
32°S (P06)	$\Delta n_{\text{C}_{\text{cal}}}$	$1.0 \pm 0.4$	Murata et al. [2007]
4°S–30°N (P10)	$\Delta n_{\text{C}_{\text{cal}}}$	$0.5 \pm 0.1$	Murata et al. [2009]
45°N	$\Delta C^*$	$0.4 \pm 0.1$	Wakita et al. [2010]
60°S–20°S (P16)	eMLR	$0.52 \pm 0.2$	Sabine et al. [2008]
20°S–20°N (P16)	eMLR	$0.28 \pm 0.1$	Sabine et al. [2008]
20°N–50°N (P16)	eMLR	$0.26 \pm 0.1$	Sabine et al. [2008]
60°S–20°S (P16, P18, and P06)	eMLR- <sup>13</sup> C	$0.63 \pm 0.15$	This study
20°S–20°N (P16 and P18)	eMLR- <sup>13</sup> C	$0.32 \pm 0.07$	This study
20°N–50°N (P16, P17, and P10)	eMLR- <sup>13</sup> C	$0.32 \pm 0.09$	This study
60°S–20°S (zonal)	MOM	0.54	This study
20°S–20°N (zonal)	MOM	0.27	This study
20°N–50°N (zonal)	MOM	0.30	This study

output from a suite of 10 ocean general circulation models that were adjusted (via air-sea CO<sub>2</sub> exchange rate) to match the historic distribution of anthropogenic CO<sub>2</sub> accumulation in the ocean. Gruber *et al.*'s meridional trend in the anthropogenic CO<sub>2</sub> inventory change generally agreed with the δ<sup>13</sup>C based trend (Figure 8) with one exception being the Southern Ocean where the mean model estimate of  $\sim 0.5 \pm 0.6 \text{ mol m}^{-2} \text{ yr}^{-1}$  south of 58°S was threefold higher than the δ<sup>13</sup>C-based estimate of  $0.14 \pm 0.04 \text{ mol m}^{-2} \text{ yr}^{-1}$ , although there was substantial uncertainty in the model estimate. A low anthropogenic CO<sub>2</sub> accumulation rate south of 60°S in the Pacific based on δ<sup>13</sup>C observations and predicted by MOM was supported by the results of Williams *et al.* [2015] who estimated an anthropogenic CO<sub>2</sub> inventory change of  $0.10 \pm 0.02 \text{ mol m}^{-2} \text{ yr}^{-1}$  by applying an MLR analysis to DIC data collected on the east-west WOCE/CLIVAR cruise S04 which crossed the entire basin along 67°S. It would be worth understanding why there was a discrepancy between model-inversion and MLR-based anthropogenic CO<sub>2</sub> accumulation rates in the Pacific Ocean south of 60°S and continued measurements of decadal scale changes in ocean δ<sup>13</sup>C and DIC in this region would help.

### 3.4. Air-Sea <sup>13</sup>CO<sub>2</sub> Exchange

The mechanism causing the δ<sup>13</sup>C of the ocean to change was air-sea CO<sub>2</sub> exchange, which transfers the fossil fuel combustion produced δ<sup>13</sup>C perturbation of the atmospheric CO<sub>2</sub> into the ocean's DIC pool. Ocean-wide, the total air-sea flux of <sup>13</sup>CO<sub>2</sub> into the ocean, should equal the DIC<sup>13</sup> inventory change (adjusted for riverine input and sedimentary loss of DIC<sup>13</sup> in the ocean). A significant advantage of using δ<sup>13</sup>C as a tracer of anthropogenic CO<sub>2</sub> changes in the ocean is that in most ocean regions the air-sea <sup>13</sup>CO<sub>2</sub> exchange rate can be accurately estimated from the measured air-sea δ<sup>13</sup>C disequilibrium so a comparison to the DIC<sup>13</sup> inventory change provides information about transport of anthropogenic CO<sub>2</sub> in the ocean interior, as discussed below.

#### 3.4.1. Air-Sea δ<sup>13</sup>C Disequilibrium

The δ<sup>13</sup>C of CO<sub>2</sub> dissolved in the surface ocean is not in isotopic equilibrium with atmospheric CO<sub>2</sub>. Due to its decade-long air-sea equilibration time, the surface ocean δ<sup>13</sup>C is primarily controlled by export of organic matter and the supply of DIC. In the industrial era, the air-sea δ<sup>13</sup>C disequilibrium is also impacted by the ongoing decrease in the δ<sup>13</sup>C of atmospheric CO<sub>2</sub>. The air-sea δ<sup>13</sup>C disequilibrium (δ<sup>13</sup>C<sub>dis</sub>) was expressed as follows:

$$\delta^{13}\text{C}_{\text{dis}}(\text{‰}) = \delta^{13}\text{C}_{\text{atm}} - (\delta^{13}\text{C}_{\text{DIC}} - \epsilon_{\text{DIC-g}}), \quad (2)$$

where δ<sup>13</sup>C<sub>DIC</sub> and δ<sup>13</sup>C<sub>atm</sub> were the δ<sup>13</sup>C of ocean DIC and atmospheric CO<sub>2</sub>, respectively, and ε<sub>DIC-g</sub> was the equilibrium fractionation between DIC and CO<sub>2</sub> gas. Determining δ<sup>13</sup>C<sub>dis</sub> required measurements of the δ<sup>13</sup>C of atmospheric CO<sub>2</sub>, δ<sup>13</sup>C of DIC, and estimates of ε<sub>DIC-g</sub> which depends primarily on sea surface temperature [Zhang *et al.*, 1995]. Using the extensive set of δ<sup>13</sup>C measurements ( $n = \sim 3600$ ) in the surface layer of the Pacific Ocean during the 1990s and 2000s from the WOCE and CLIVAR cruises (Figure 1), container ship cruises between 2004 and 2015 [Quay *et al.*, 2003, 2009, and unpublished data] and time series at HOT and DP the δ<sup>13</sup>C<sub>dis</sub> can be estimated with a mean uncertainty of  $\sim \pm 0.10\text{‰}$ .

δ<sup>13</sup>C<sub>dis</sub> ranged from  $-2$  to  $+2 \text{‰}$  with a clear latitudinal trend (Figure 9) that was mainly the result of the temperature dependence of ε<sub>DIC-g</sub>, as the sea surface δ<sup>13</sup>C only varied by  $\sim 1\text{‰}$  (Figure 2). In the equatorial and subtropical Pacific Ocean, where δ<sup>13</sup>C<sub>dis</sub> was negative, air-sea CO<sub>2</sub> gas exchange acted to decrease the δ<sup>13</sup>C of the surface ocean whereas at high latitudes poleward of  $\sim 50^\circ$ , where δ<sup>13</sup>C<sub>dis</sub> was positive, gas exchange acted to increase δ<sup>13</sup>C. δ<sup>13</sup>C<sub>dis</sub> has remained essentially constant between the 1990s and 2000s for most of the Pacific Ocean. Basin-wide, the area-weighted mean δ<sup>13</sup>C<sub>dis</sub>, equaled  $-1.21 \pm 0.10\text{‰}$  in the 1990s (mean data year 1994) and  $-1.28 \pm 0.10\text{‰}$  in the 2000s (mean data year 2008). This small temporal change in δ<sup>13</sup>C<sub>dis</sub> ( $-0.05 \pm 0.13\text{‰ decade}^{-1}$ ) was expected as the δ<sup>13</sup>C decrease rate of the surface ocean ( $-0.20\text{‰ decade}^{-1}$ ) has not fully kept pace with the atmospheric δ<sup>13</sup>C change ( $-0.27\text{‰ decade}^{-1}$ ). MOM predicted a similar latitudinal trend in δ<sup>13</sup>C<sub>dis</sub> but with a slightly lower basin mean value of  $-1.35\text{‰}$  in 1995 (Figure 9).

The current (contemporary) air-sea δ<sup>13</sup>C<sub>dis</sub> measured or predicted by models is a result of preindustrial conditions and the anthropogenic perturbation. Without direct measurements of the preindustrial surface ocean δ<sup>13</sup>C the preindustrial δ<sup>13</sup>C<sub>dis</sub> conditions must be estimated from models or, where available, proxy δ<sup>13</sup>C records [e.g., Bohm *et al.*, 2002]. Here the output from MOM was used to estimate the air-sea δ<sup>13</sup>C disequilibrium during preindustrial times in the Pacific Ocean. Because MOM predicted anthropogenic δ<sup>13</sup>C and

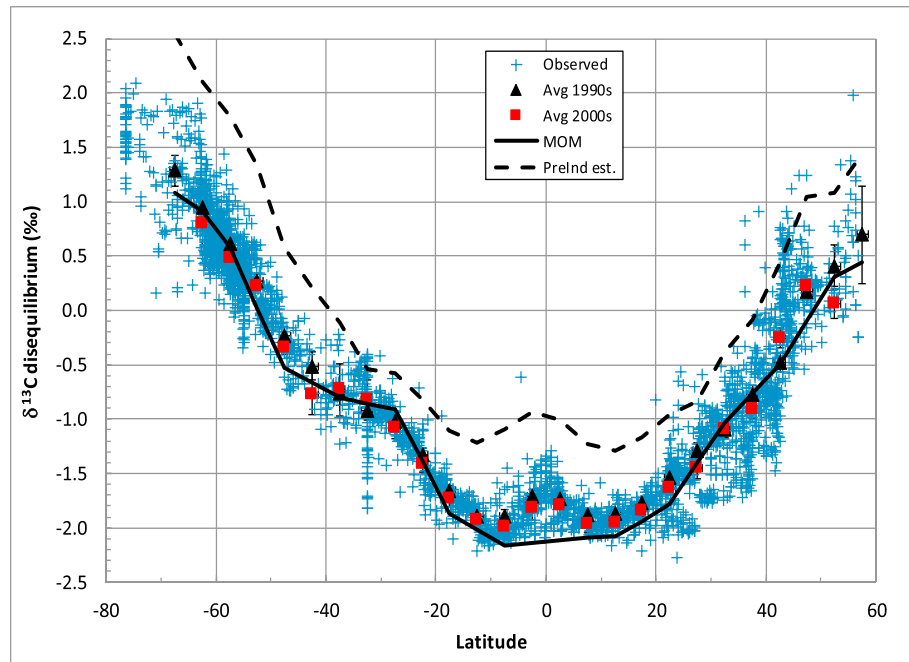


**Figure 9.** The latitudinal trends in air-sea  $\delta^{13}\text{C}$  disequilibrium ( $\delta^{13}\text{C}_{\text{atm}} - [\delta^{13}\text{C}_{\text{DIC}} - \epsilon_{\text{DIC-g}}]$ ) in the 1990s and 2000s in the Pacific Ocean. Zonally averaged sea surface temperatures were used to calculate  $\epsilon_{\text{DIC-g}}$  [Zhang *et al.*, 1995]. MOM predicted zonally averaged  $\delta^{13}\text{C}$  disequilibrium in 1995 (solid line) and estimated  $\delta^{13}\text{C}$  disequilibrium for Pacific Ocean during preindustrial times (dashed line).

$\text{CO}_2$  inventory changes that agreed well with the  $\delta^{13}\text{C}$  observations (Figures 7 and 8), it was reasonable to expect that the model-predicted change in air-sea  $\delta^{13}\text{C}$  disequilibrium was representative of the actual change. The model-predicted change was likely more accurate than its absolute values (of either the preindustrial or contemporary  $\delta^{13}\text{C}_{\text{dis}}$ ). Thus, a mean basin preindustrial  $\delta^{13}\text{C}_{\text{dis}}$  of  $-0.46\text{‰}$  was estimated by subtracting the modeled disequilibrium change ( $-0.75\text{‰}$ ) from the measured mean contemporary  $\delta^{13}\text{C}_{\text{dis}}$  of  $-1.21\text{‰}$  in the 1990s (Figure 9).

### 3.4.2. Air-Sea $^{13}\text{CO}_2$ Flux

The current (contemporary) air-sea  $^{13}\text{CO}_2$  flux ( $F_{13\text{CO}_2}$ ) was expressed as follows:

$$F_{13\text{CO}_2} = k \cdot \alpha_k \cdot \gamma \cdot \alpha_{\text{sol}} \cdot (\text{pCO}_{2\text{atm}} \cdot R_{\text{atm}} - \text{pCO}_{2\text{oc}} \cdot R_{\text{DIC}} \cdot \alpha_{\text{DIC-g}}) \quad (3a)$$

where  $k$  is the gas transfer (or piston) velocity,  $\gamma$  was the solubility of  $\text{CO}_2$  in seawater [Weiss, 1974], and  $\text{pCO}_{2\text{atm}}$  and  $\text{pCO}_{2\text{oc}}$  are the partial pressures of  $\text{CO}_2$  in air and seawater, respectively.  $R_{\text{atm}}$  and  $R_{\text{DIC}}$  represent the measured  $^{13}\text{C}/^{12}\text{C}$  ratios of  $\text{CO}_2$  in air and seawater DIC, respectively, where  $R = (\delta^{13}\text{C}/1000 + 1) \cdot R_{\text{PDB}}$  and  $\alpha_k$  was the kinetic fractionation factor for  $\text{CO}_2$  diffusion through the boundary layer, and  $\alpha_{\text{sol}}$  was the equilibrium fractionation factor for  $\text{CO}_2$  gas dissolution in seawater [Zhang *et al.*, 1995]. It was assumed that  $^{12}\text{CO}_2$  adequately represents (98.9%) bulk  $\text{CO}_2$ .

The impact of air-sea  $^{13}\text{CO}_2$  flux on the  $^{13}\text{C}/^{12}\text{C}$  of the DIC in the ocean can be separated into two components [Quay *et al.*, 2007], i.e., gross air-sea  $\text{CO}_2$  exchange flux operating on the air-sea  $\delta^{13}\text{C}$  disequilibrium and the net flux of  $\text{CO}_2$  carrying with it the  $\delta^{13}\text{C}$  of dissolved  $\text{CO}_2$  gas. These effects can be distinguished by expanding equation (3a):

$$F_{13\text{CO}_2} = k \cdot \alpha_k \cdot \gamma \cdot \alpha_{\text{sol}} \cdot R_{\text{atm}} \cdot [\text{pCO}_{2\text{atm}} \cdot (1 - 1/R_{\text{dis}}) + \Delta\text{pCO}_2/R_{\text{dis}}] \quad (3b)$$

where  $R_{\text{dis}}$  equals  $R_{\text{atm}}/(R_{\text{DIC}} \cdot \alpha_{\text{DIC-g}})$  and represents the  $^{13}\text{C}/^{12}\text{C}$  disequilibrium between atmosphere and surface ocean and  $\Delta\text{pCO}_2$  equals  $\text{pCO}_{2\text{atm}} - \text{pCO}_{2\text{oc}}$ . The first term on the right of equation (3b) represents the portion of air-sea  $^{13}\text{CO}_2$  flux resulting from gross  $\text{CO}_2$  gas exchange, and the second term was the portion due

to net CO<sub>2</sub> gas exchange. The air-sea <sup>13</sup>CO<sub>2</sub> flux, approximated in per mil notation (‰ mol m<sup>-2</sup> decade<sup>-1</sup>), was

$$F_{13\text{CO}_2} = k \cdot \gamma \cdot p\text{CO}_{2\text{atm}} \cdot (\delta^{13}\text{C}_{\text{dis}}) + k \cdot \gamma \cdot \Delta p\text{CO}_2 \cdot (\delta^{13}\text{C}_{\text{atm}} - \delta^{13}\text{C}_{\text{dis}} + \varepsilon_{\text{sol}} + \varepsilon_k) \quad (4)$$

where  $\delta^{13}\text{C}_{\text{dis}} (\text{‰}) = (R_{\text{dis}} - 1) \cdot 1000$ ,  $\varepsilon_{\text{sol}} (\text{‰}) = (\alpha_{\text{sol}} - 1) \cdot 1000$  and  $\varepsilon_k (\text{‰}) = (\alpha_k - 1) \cdot 1000$ .

Separation of the total air-sea <sup>13</sup>CO<sub>2</sub> flux into gross and net components was useful because it distinguished the effect that air-sea CO<sub>2</sub> exchange had on the  $\delta^{13}\text{C}$  of the ocean even if there were no net CO<sub>2</sub> uptake and, notably, provided a means to estimate the net ocean uptake of anthropogenic CO<sub>2</sub> without the need to measure  $\Delta p\text{CO}_2$ . In the simplest situation, i.e., no net DIC<sup>13</sup> transport or riverine flux into the region, the DIC<sup>13</sup> inventory change rate must equal the air-sea <sup>13</sup>CO<sub>2</sub> flux:

$$\text{DIC} \cdot \Delta R_{\text{DIC}} + R_{\text{DIC}} \cdot \Delta \text{DIC} = k \cdot \alpha_k \cdot \gamma \cdot \alpha_{\text{sol}} \cdot R_{\text{atm}} \cdot [p\text{CO}_{2\text{atm}} \cdot (1 - 1/R_{\text{dis}}) + \Delta p\text{CO}_2 / R_{\text{dis}}] \quad (5)$$

Rearranging equation (5) and noting that the  $\Delta \text{DIC}$  inventory change rate equals the net air-sea CO<sub>2</sub> flux under these conditions the net air-sea CO<sub>2</sub> flux was expressed as follows:

$$\begin{aligned} \text{Net contemporary CO}_2 \text{ uptake} = \\ (\text{DIC}_t \cdot \Delta R_{\text{DIC}} - k \cdot \alpha_k \cdot \gamma \cdot \alpha_{\text{sol}} \cdot p\text{CO}_{2\text{atm}} \cdot R_{\text{atm}} \cdot [1 - 1/R_{\text{dis}}]) / (R_{\text{atm}} \cdot \alpha_k \cdot \alpha_{\text{sol}} / R_{\text{dis}} - R_{\text{DIC}}) \end{aligned} \quad (6)$$

Thus, an estimate of the net contemporary CO<sub>2</sub> uptake rate by the ocean can be obtained by a comparison of DIC<sup>13</sup> inventory change rate to the gross air-sea <sup>13</sup>CO<sub>2</sub> flux. If the DIC<sup>13</sup> inventory change exceeds the gross <sup>13</sup>CO<sub>2</sub> flux then there must be net uptake of CO<sub>2</sub> to offset this imbalance (and vice versa). As DIC transport via ocean currents and mixing impact the distribution of contemporary DIC and DIC<sup>13</sup>, the rate of CO<sub>2</sub> uptake calculated by using equation (6) included both net transport and net air-sea fluxes and assumed that the CO<sub>2</sub> transferred by both processes had the same isotopic composition.

However, regionally the contemporary CO<sub>2</sub> uptake rate is not equivalent to the anthropogenic CO<sub>2</sub> uptake rate. One can view the contemporary ocean DIC<sup>13</sup> budget as composed of preindustrial and anthropogenic components. In preindustrial times steady state was maintained by the total transport (representing all inputs or outputs) of DIC<sup>13</sup> into a region offsetting the total (gross + net) air-sea <sup>13</sup>CO<sub>2</sub> flux. The anthropogenic DIC<sup>13</sup> transport and air-sea <sup>13</sup>CO<sub>2</sub> flux are superimposed on the preindustrial conditions. Thus, in order to estimate anthropogenic CO<sub>2</sub> uptake from recently measured (contemporary) air-sea <sup>13</sup>CO<sub>2</sub> flux and DIC<sup>13</sup> inventory change one has to account for the preindustrial air-sea <sup>13</sup>CO<sub>2</sub> flux and DIC<sup>13</sup> transport into or out of the region. Here we used output from MOM to estimate the preindustrial air-sea  $\delta^{13}\text{C}$  disequilibrium in the Pacific Ocean (Figure 9), as discussed above, and then calculated the preindustrial air-sea <sup>13</sup>CO<sub>2</sub> flux on 5° latitude intervals. The anthropogenic CO<sub>2</sub> uptake rate was estimated by comparing contemporary DIC<sup>13</sup> inventory change to difference between the contemporary and preindustrial air-sea <sup>13</sup>CO<sub>2</sub> flux as shown in equation (7):

$$\begin{aligned} \text{Anthropogenic CO}_2 \text{ uptake} = & ([\text{DIC}_t \cdot \Delta R_{\text{DIC}} - \gamma \cdot \alpha_{\text{sol}} \cdot p\text{CO}_{2\text{atm}} \cdot R_{\text{atm}} \cdot (1 - 1/R_{\text{dis}})]_{\text{con}} \\ & + [k \cdot \alpha_k \cdot \gamma \cdot \alpha_{\text{sol}} \cdot p\text{CO}_{2\text{atm}} \cdot R_{\text{atm}} \cdot (1 - 1/R_{\text{dis}})]_{\text{pre}}) / (R_{\text{atm}} \cdot \alpha_k \cdot \alpha_{\text{sol}} / R_{\text{dis}} - R_{\text{DIC}})_{\text{con}}, \end{aligned} \quad (7)$$

where con represent contemporary and pre represents preindustrial conditions. Again, this estimate of anthropogenic CO<sub>2</sub> uptake represented anthropogenic CO<sub>2</sub> added to a region by both net air-sea CO<sub>2</sub> flux and ocean transport and assumed that the CO<sub>2</sub> transferred by both processes had the same isotopic composition.

### 3.4.3. Anthropogenic CO<sub>2</sub> Uptake Rates Based on Measured $\delta^{13}\text{C}$ Changes

A comparison between ocean DIC<sup>13</sup> inventory change and gross air-sea <sup>13</sup>CO<sub>2</sub> flux provided a means to estimate regional ocean uptake rates of atmospheric CO<sub>2</sub> that was independent of estimates based on measured  $\Delta p\text{CO}_2$ . In this sense these  $\delta^{13}\text{C}$ -based regional estimates provide additional constraints for validation of ocean model-based anthropogenic CO<sub>2</sub> uptake rates. Although the <sup>13</sup>C-based estimates of ocean CO<sub>2</sub> uptake rates had significant uncertainties, as discussed below, they exhibited a meridional pattern and magnitude that agreed with estimates based on model inversions and forward simulations of the anthropogenic CO<sub>2</sub> perturbation in the Pacific Ocean [e.g., Gruber *et al.*, 2009; Khatiwala *et al.*, 2013].

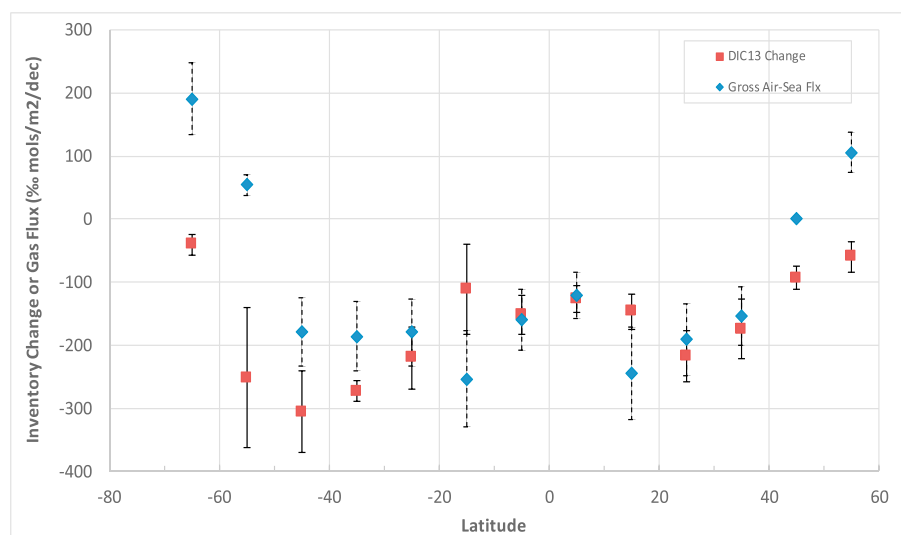


**Figure 10.** Latitudinal trends in the DIC<sup>13</sup> inventory change and gross air-sea <sup>13</sup>CO<sub>2</sub> flux (% mol m<sup>-2</sup> decade<sup>-1</sup>). Values represent means (±SE) over 10° latitude intervals.

The latitudinal trend in the gross contemporary <sup>13</sup>CO<sub>2</sub> flux was primarily a result of the latitudinal trends in the air-sea <sup>13</sup>C/<sup>12</sup>C disequilibrium ( $\delta^{13}\text{C}_{\text{dis}}$ ) and partly a result of latitudinal variations in  $k$ , which in turn depends on wind speed [Ho *et al.*, 2006] and CO<sub>2</sub> solubility ( $\gamma$ ) which about doubles with a 20°C decrease in temperature [Weiss, 1974]. The gross <sup>13</sup>CO<sub>2</sub> flux ranged from  $-250\%$  mol m<sup>-2</sup> decade<sup>-1</sup> in the tropical ocean (20°S to 20°N) to  $+200\%$  mol m<sup>-2</sup> decade<sup>-1</sup> in the Southern Ocean (south of 60°S) with the transition from negative to positive  $\delta^{13}\text{C}_{\text{dis}}$  values occurring at  $\sim 50^\circ$  N and S (Figure 10). In comparison, the DIC<sup>13</sup> inventory change rate ranged from  $-40$  to  $-300\%$  mol m<sup>-2</sup> decade<sup>-1</sup> (Figure 10) and followed the trend in depth-integrated  $\delta^{13}\text{C}$  change (Figure 7), where the greatest change occurred between 30°S and 60°S and smaller changes occurred in the equatorial Pacific, subpolar North Pacific and Southern Ocean (Figure 10). Generally, the similar latitudinal trend and magnitudes of the gross air-sea <sup>13</sup>CO<sub>2</sub> flux and DIC<sup>13</sup> inventory change underscored the dominant impact of air-sea CO<sub>2</sub> exchange on recent  $\delta^{13}\text{C}$  changes in the Pacific Ocean.

In regions where the gross contemporary air-sea <sup>13</sup>CO<sub>2</sub> flux exceeded (more negative value) the DIC<sup>13</sup> inventory change since the 1990s either there was net air-sea CO<sub>2</sub> outgassing and/or ocean transport removed anthropogenic DIC<sup>13</sup> from the region. This is the situation at the edges (15°N and S) of the equatorial Pacific (Figure 10). Contrastingly, in regions where the gross air-sea <sup>13</sup>CO<sub>2</sub> flux was smaller (more positive value) than the DIC<sup>13</sup> inventory change there was either net uptake of atmospheric CO<sub>2</sub> and/or horizontal transport added anthropogenic DIC<sup>13</sup> to this region. This is the situation at high latitudes in the South (40°S and 70°S) and North (north of 40°N) Pacific (Figure 10); in both these regions despite cold surface waters resulting in air-sea CO<sub>2</sub> exchange enriching the  $\delta^{13}\text{C}$  of surface DIC, a  $\delta^{13}\text{C}$  decrease in the DIC inventory was observed.

There was a clear meridional trend in the  $\delta^{13}\text{C}$ -based estimates of contemporary net air-sea CO<sub>2</sub> flux (Figure 11) determined by using equation (6) which represents CO<sub>2</sub> uptake via air-sea exchange and ocean transport, as discussed above. Overall, there was net CO<sub>2</sub> uptake poleward of 20° and net CO<sub>2</sub> outgassing equatorward of 20°. The highest CO<sub>2</sub> uptake rates occurred between 40°S and 70°S where the difference between DIC<sup>13</sup> inventory change and gross <sup>13</sup>CO<sub>2</sub> flux was greatest (Figure 10). The highest CO<sub>2</sub> outgassing rates occurred between 10° and 20° (N and S) where the gross <sup>13</sup>CO<sub>2</sub> flux significantly exceeded the DIC<sup>13</sup> inventory change. In the subtropical North Pacific (20–40°N) and equatorial Pacific (10°S to 10°N) the net CO<sub>2</sub> uptake was not significantly different from zero given the uncertainty of the estimates. In comparison, estimates of the contemporary net CO<sub>2</sub> flux based on  $\Delta\text{pCO}_2$  [Takahashi *et al.*, 2009], model inversions [Gruber *et al.*, 2009], and output from MOM showed similar meridional trends to the  $\delta^{13}\text{C}$ -based estimates, i.e., net CO<sub>2</sub> uptake poleward of 20° and outgassing in the equatorial ocean. Although the magnitude of the  $\delta^{13}\text{C}$ -based and model-based contemporary CO<sub>2</sub> uptake rates were generally in good agreement, the

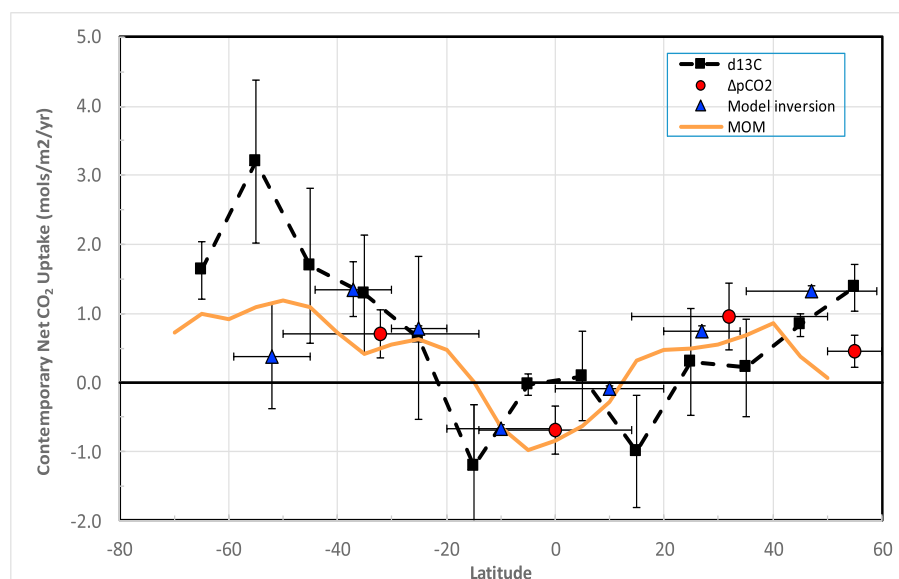


**Figure 11.** Latitudinal trend in rate of contemporary net air-sea CO<sub>2</sub> flux estimated from difference between DIC<sup>13</sup> inventory change and gross air-sea <sup>13</sup>CO<sub>2</sub> flux (dashed line), observed ΔpCO<sub>2</sub> [Takahashi *et al.*, 2009], and predicted by ocean model inversion [Gruber *et al.*, 2009] and MOM (solid line).

one notable exception was between 50°S and 60°S where the δ<sup>13</sup>C-based estimates significantly exceeded MOM and model inversion-based estimates (Figure 11).

A basin-wide (north of 60°S) contemporary CO<sub>2</sub> uptake rate of  $0.38 \pm 0.74 \text{ mol C m}^{-2} \text{ yr}^{-1}$  ( $0.74 \pm 1.5 \text{ Pg yr}^{-1}$ ) was estimated by area-weighting the regional uptake rates (Figure 11). The large error in δ<sup>13</sup>C-based net CO<sub>2</sub> uptake rate was a result of the DIC<sup>13</sup> inventory change being dominated by the gross <sup>13</sup>CO<sub>2</sub> flux rate, where both rate estimates had significant uncertainties. Note that about half of the estimated basin-wide net CO<sub>2</sub> uptake rate ( $0.39 \text{ Pg yr}^{-1}$ ) occurred between 50°S and 60°S, which yielded a rate of  $0.37 \pm 1.3 \text{ Pg yr}^{-1}$  north of 50°S. In comparison, Takahashi *et al.*'s [2009] ΔpCO<sub>2</sub>-based estimate of net air-sea contemporary (1995) was  $0.46 \pm 0.24 \text{ Pg yr}^{-1}$  for the Pacific Ocean (north of 50°S). MOM predicted a contemporary net air-sea CO<sub>2</sub> flux of  $0.36 \text{ Pg yr}^{-1}$ , whereas a suite of ocean models with air-sea CO<sub>2</sub> exchange rates tuned to account for the industrial era anthropogenic CO<sub>2</sub> distribution in the ocean [Gruber *et al.*, 2009] yielded a mean contemporary air-sea CO<sub>2</sub> uptake rate of  $\sim 0.7 \pm 0.2 \text{ Pg yr}^{-1}$  (north of  $\sim 60^\circ\text{S}$ ). The difference between MOM and the model-inversion results was due to differing preindustrial conditions, as discussed below.

The contemporary CO<sub>2</sub> uptake rate was not equivalent to the anthropogenic CO<sub>2</sub> uptake rate because of the preindustrial conditions. Riverine organic carbon input to the global ocean in excess of sedimentation loss implied a  $\sim 0.3 \text{ Pg yr}^{-1}$  CO<sub>2</sub> outgassing at steady state [Sarmiento and Sundquist, 1992] of which about half was estimated to occur in the Pacific Ocean [Gruber *et al.*, 2009]. An ensemble of ocean model inversions yielded a small net preindustrial outgassing of  $\sim 0.10 \pm 0.04 \text{ Pg yr}^{-1}$  for the Pacific Ocean excluding outgassing caused by riverine DIC input [Mikaloff Fletcher *et al.*, 2007]. In contrast, MOM predicted a significantly stronger preindustrial CO<sub>2</sub> outgassing rate of  $0.45 \text{ Pg yr}^{-1}$  for the Pacific (excluding riverine DIC input) which was dominated by the equatorial Pacific ( $0.60 \text{ Pg yr}^{-1}$ ). The preindustrial CO<sub>2</sub> flux in MOM is likely too strong as coarse-resolution ocean models significantly overestimate upwelling of nutrient and CO<sub>2</sub>-rich waters in the equatorial Pacific [Toggweiler *et al.*, 1989; Matear and Holloway, 1995; Aumont *et al.*, 1999]. In MOM, the equatorial Pacific is a major site where abyssal CO<sub>2</sub> is returned to the atmosphere resulting in significant loss of preindustrial CO<sub>2</sub> from the Pacific Basin.

The magnitude of the preindustrial air-sea CO<sub>2</sub> outgassing flux is important because if it was small then the magnitude of the anthropogenic air-sea CO<sub>2</sub> flux would be similar to the contemporary net CO<sub>2</sub> air-sea flux whereas if it was large the anthropogenic CO<sub>2</sub> flux would be significantly larger than the

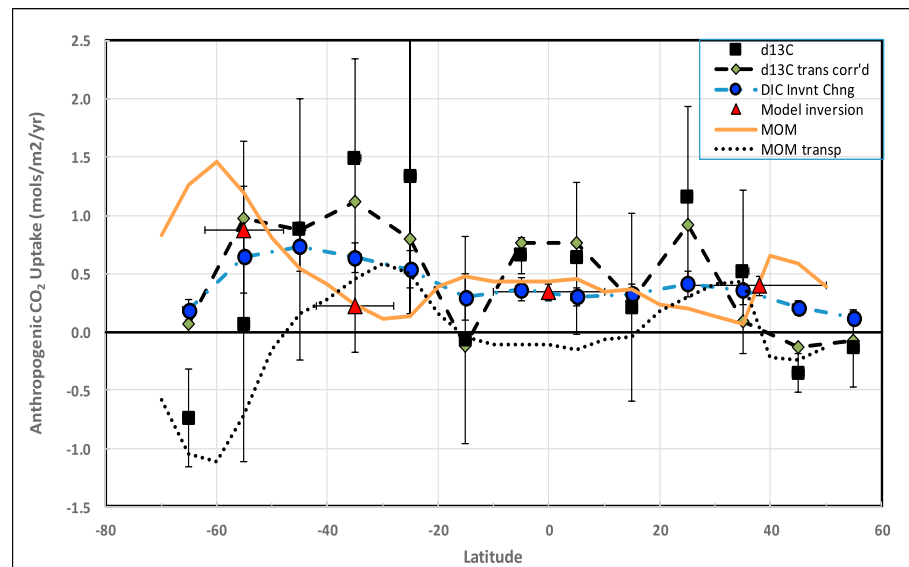


**Figure 12.** Latitudinal trend in anthropogenic  $\text{CO}_2$  uptake (positive value implies ocean uptake) estimated from difference between  $\text{DIC}^{13}$  inventory change and air-sea  $^{13}\text{C}$  flux (including ocean transport) and air-sea anthropogenic  $\text{CO}_2$  uptake predicted by ocean model inversion [Gruber *et al.*, 2009] and MOM (solid line). MOM predicted transport of anthropogenic  $\text{CO}_2$  (dotted line) and  $\delta^{13}\text{C}$ -based estimates of air-sea anthropogenic  $\text{CO}_2$  uptake after correcting for transport using output from MOM (dashed line). Trend in anthropogenic  $\text{CO}_2$  inventory change estimated from measured  $\text{DIC}^{13}$  inventory change and RC is included for comparison.

contemporary air-sea flux. For MOM, the estimated anthropogenic air-sea  $\text{CO}_2$  flux at  $0.80 \text{ Pg yr}^{-1}$  was a result of the contemporary  $\text{CO}_2$  uptake at  $0.36 \text{ Pg yr}^{-1}$  being superimposed on a preindustrial  $\text{CO}_2$  outgassing of  $-0.44 \text{ Pg yr}^{-1}$ . In contrast the model inversion approach of Gruber *et al.* [2009] yields an anthropogenic air-sea  $\text{CO}_2$  flux for the Pacific of  $0.68 \pm 0.15 \text{ Pg yr}^{-1}$  that was similar to the contemporary flux of  $0.70 \pm 0.13 \text{ Pg yr}^{-1}$  because of a negligible basin-wide net preindustrial air-sea  $\text{CO}_2$  flux.

To calculate the net anthropogenic  $\text{CO}_2$  uptake rate based on  $\delta^{13}\text{C}$  changes (equation (7)) one needed to account for the preindustrial air-sea  $^{13}\text{C}$  flux which was estimated by using the industrial era change in air-sea  $\delta^{13}\text{C}$  disequilibrium predicted by MOM, as discussed above. There were notable differences between the  $\delta^{13}\text{C}$ -based estimates of anthropogenic (Figure 12) and contemporary net  $\text{CO}_2$  uptake rates (Figure 11). In the tropical Pacific there was net anthropogenic  $\text{CO}_2$  uptake despite being a region of net contemporary  $\text{CO}_2$  degassing. Poleward of  $40^\circ$  the estimated net anthropogenic  $\text{CO}_2$  uptake rates were significantly lower than contemporary rates. In the subtropical gyres, in contrast, estimated anthropogenic  $\text{CO}_2$  uptake rates were higher than contemporary rates. Basin-wide, the estimated anthropogenic  $\text{CO}_2$  uptake rate, increased to  $1.2 \pm 1.5 \text{ Pg yr}^{-1}$  (north of  $60^\circ\text{S}$ ) compared to a contemporary  $\text{CO}_2$  uptake rate of  $0.73 \pm 1.5$ . In comparison, MOM- and model-inversion [Gruber *et al.*, 2009]-based estimates of basin-wide anthropogenic air-sea  $\text{CO}_2$  uptake were  $0.8$  and  $0.7 \pm 0.15 \text{ Pg yr}^{-1}$ , respectively.

When comparing the  $\delta^{13}\text{C}$ -based anthropogenic  $\text{CO}_2$  uptake rates to those predicted by MOM there are some discrepancies. In regions of upwelling and Ekman divergence (south of  $50^\circ\text{S}$  and subarctic) the  $\delta^{13}\text{C}$ -based rates were lower than model rates whereas in region of downwelling and Ekman convergence (subtropics) the  $\delta^{13}\text{C}$ -based rates were higher than model rates. At first glance this may have been surprising as the meridional trends in  $\delta^{13}\text{C}$ - and model- based estimates of anthropogenic  $\text{CO}_2$  inventory change agreed well (Figure 8). The explanation involved ocean transport. As noted above, the  $\delta^{13}\text{C}$ -based anthropogenic  $\text{CO}_2$  uptake rates calculated by using equation (7) represent the net  $\text{CO}_2$  uptake or loss resulting from both air-sea  $\text{CO}_2$  flux and ocean  $\text{CO}_2$  transport. Although transport of anthropogenic  $\text{CO}_2$  was likely small on a basin-wide scale for the Pacific Ocean (i.e., estimated at  $\sim 0.1 \text{ Pg yr}^{-1}$  at  $60^\circ\text{S}$  by MOM) it was substantial on regional scales. Using output from MOM, the meridional trend of anthropogenic  $\text{CO}_2$  input and loss resulting from transport was essentially a mirror image of the net anthropogenic air-sea  $\text{CO}_2$  flux (Figure 12). In upwelling regions Ekman transport exported anthropogenic  $\text{CO}_2$  out of the region, whereas in downwelling

regions Ekman transport imported anthropogenic CO<sub>2</sub> into the region. MOM's results explained why the  $\delta^{13}\text{C}$ -based anthropogenic uptake rates underestimated air-sea CO<sub>2</sub> uptake in upwelling regions and overestimate them in downwelling regions. To illustrate the importance of transport-based redistribution of anthropogenic CO<sub>2</sub> in the Pacific Ocean, we corrected the  $\delta^{13}\text{C}$ -based estimates of anthropogenic CO<sub>2</sub> uptake for transport effects using transport estimates from MOM. The meridional trend in the transport corrected  $\delta^{13}\text{C}$ -based air-sea anthropogenic CO<sub>2</sub> flux agreed significantly better with model estimates of anthropogenic CO<sub>2</sub> uptake and the  $\delta^{13}\text{C}$ -based anthropogenic CO<sub>2</sub> inventory change (Figure 12). These results reveal the importance of ocean transport in redistributing anthropogenic CO<sub>2</sub> in the Pacific Ocean and highlight the utility of  $\delta^{13}\text{C}$  as a tracer to track this redistribution and help validate model predictions of anthropogenic CO<sub>2</sub> accumulation.

#### 4. Summary

A significant decrease in the  $\delta^{13}\text{C}$  of DIC between the 1990s WOCE and 2000s CLIVAR measurements across the entire Pacific Ocean was clearly detectable. The  $\delta^{13}\text{C}$  of DIC in the surface layer of the Pacific Ocean has decreased at about  $0.20 \pm 0.06\text{‰ decade}^{-1}$  which was slightly slower than the  $-0.27\text{‰ decade}^{-1}$  rate for atmospheric CO<sub>2</sub>. A high surface ocean  $\delta^{13}\text{C}$  decrease rate of  $-0.28 \pm 0.02\text{‰ decade}^{-1}$  and DIC increase of  $14 \mu\text{mol kg}^{-1} \text{ decade}^{-1}$  were observed in the Drake Passage which suggests that this region of the Southern Ocean has experienced high accumulation rates of anthropogenic CO<sub>2</sub>. Using an MLR-based approach to isolate the anthropogenic component of the  $\delta^{13}\text{C}$  changes at depth yielded a basin-wide depth-integrated rate of  $-83 \pm 20\text{‰ m decade}^{-1}$ , about half the rate of  $-150 \pm 38\text{‰ m decade}^{-1}$  in the North Atlantic between the 1990s and 2000s [Quay *et al.*, 2007] but similar to the global ocean average rate of  $-65 \pm 33\text{‰ m decade}^{-1}$  [Quay *et al.*, 2003]. The DIC<sup>13</sup> inventory change resulted primarily (~85%) from gross air-sea CO<sub>2</sub> exchange rate acting on the basin-wide air-sea  $\delta^{13}\text{C}$  disequilibrium of  $-1.2\text{‰}$  and, secondarily, from net ocean uptake of anthropogenic CO<sub>2</sub>. The similar magnitudes of the depth-integrated DIC<sup>13</sup> inventory change rate and the air-sea <sup>13</sup>CO<sub>2</sub> flux in the Pacific Ocean differed distinctly from the situation in the North Atlantic Ocean where the DIC<sup>13</sup> inventory change was about twice the air-sea <sup>13</sup>CO<sub>2</sub> flux. There were clear latitudinal trends in the depth-integrated anthropogenic  $\delta^{13}\text{C}$  change with maximum occurring between 30°S and 60°S and minima in the Southern Ocean (south of 60°S) and subpolar N. Pacific.

The depth-integrated  $\delta^{13}\text{C}$  changes, combined with estimates of the ratio of anthropogenic  $\delta^{13}\text{C}$  to DIC change, yielded an estimate of the anthropogenic CO<sub>2</sub> accumulation rate of  $0.82 \pm 0.26 \text{ Pg yr}^{-1}$  for the Pacific (60°S–60°N) in the Pacific Ocean between the 1990s and 2000s. The meridional trend in  $\delta^{13}\text{C}$ -based anthropogenic CO<sub>2</sub> inventory change showed a maximum between 60°S–30°S and minima in the Southern Ocean (south of 60°S) and subpolar North Pacific that agreed well with previous observation- and model-based estimates.

Differences between DIC<sup>13</sup> inventory changes in the water column and gross air-sea <sup>13</sup>CO<sub>2</sub> fluxes at the sea surface yielded estimates of the net contemporary air-sea CO<sub>2</sub> uptake rate that were independent of  $\Delta\text{pCO}_2$  measurements and indicate net CO<sub>2</sub> outgassing in the equatorial Pacific and net CO<sub>2</sub> uptake poleward of 20° which generally agreed in magnitude and meridional trend with estimates based on a  $\Delta\text{pCO}_2$  compilation [Takahashi *et al.*, 2009] and ocean models. To estimate anthropogenic CO<sub>2</sub> uptake rates using  $\delta^{13}\text{C}$  tracer required an estimate of preindustrial surface ocean  $\delta^{13}\text{C}$  conditions which was obtained from an ocean model's predicted change in  $\delta^{13}\text{C}$  disequilibrium during the industrial era. The  $\delta^{13}\text{C}$ -based estimates of anthropogenic CO<sub>2</sub> uptake were highest between 30°S and 60°S and lowest in the subpolar North Pacific and south of 60°S. A comparison of the meridional trends in anthropogenic DIC<sup>13</sup> inventory changes and air-sea <sup>13</sup>CO<sub>2</sub> flux indicates that regionally ocean transport of anthropogenic CO<sub>2</sub> plays a major role in controlling the distribution of anthropogenic CO<sub>2</sub> accumulation within the Pacific Ocean basin.

The results presented here demonstrate that the clearly detectable anthropogenic  $\delta^{13}\text{C}$  change coupled with the ability to accurately measure the air-sea  $\delta^{13}\text{C}$  disequilibrium make  $\delta^{13}\text{C}$  a powerful tracer of anthropogenic CO<sub>2</sub> uptake and redistribution in the ocean on regional scales and decadal time intervals.

## Acknowledgments

We thank all the personnel on the WOCE and CLIVAR, Gould, and HOT cruises who collected the  $\delta^{13}\text{C}$  samples and in the laboratories (NOSAMS, UW, and JAMSTEC) where the samples were analyzed especially Johnny Stutsman, Mark Haught, and many undergraduates who helped with the  $\delta^{13}\text{C}$  analyses at the UW. The  $\delta^{13}\text{C}$  data collected during WOCE and CLIVAR are available in the GLODAP database (<http://cdiac.ornl.gov/oceans/GLODAPv2/>). The surface  $\delta^{13}\text{C}$  data have been submitted to BCO-DMO (<http://www.bco-dmo.org/data>). This study was supported by NSF OCE 1259055 and OCE 1356756 (P.Q. and R.S.). Collection and analysis of Drake Passage samples were supported by NSF PLR 1341647, NSF PLR 1543457, AOAS 0944761, and AOAS 0636975 (C.S. and D.M.). Email contact: pqduay@uw.edu.

## References

- Aumont, O., J. C. Orr, P. Monfray, G. Madec, and E. Maier-Reimer (1999), Nutrient trapping in the equatorial Pacific: The ocean circulation solution, *Global Biogeochem. Cycles*, *13*, 351–369, doi:10.1029/1998GB900012.
- Bohm, F., A. Haase-Schramm, A. Eisenhauer, W. C. Dullo, M. M. Joachimski, H. Lehnert, and J. Reitner (2002), Evidence for preindustrial variations in the marine surface water carbonate system from coralline sponges, *Geochem. Geophys. Geosyst.*, *3*(3), doi:10.1029/2001GC000264.
- Francey, R. M., A. J. Key, C. E. Allison, D. M. Etheridge, C. M. Trudinger, I. G. Enting, M. Leuenberger, J. L. Langenfelds, E. Michel, and L. P. Steele (1999), A 100-year high precision record of  $\delta^{13}\text{C}$  in atmospheric  $\text{CO}_2$ , *Tellus, Ser. B*, *51*, 170–193.
- Friis, K., A. Körtzinger, J. Pätzsch, and D. W. R. Wallace (2005), On the temporal increase of anthropogenic  $\text{CO}_2$  in the subpolar North Atlantic, *Deep Sea Res., Part I*, *52*, 681–698.
- Gent, P., and J. C. McWilliams (1990), Isopycnal mixing in ocean circulation models, *J. Phys. Oceanogr.*, *20*, 150–155.
- Gnanadesikan, A., J. P. Dunne, R. M. Key, K. Matsumoto, J. L. Sarmiento, R. D. Slater, and P. S. Swathi (2004), Oceanic ventilation and biogeochemical cycling: Understanding the physical mechanisms that produce realistic distributions of tracers and productivity, *Global Biogeochem. Cycles*, *18*, GB4010, doi:10.1029/2003GB002097.
- Gruber, N., C. D. Keeling, and N. Bates (2002), Interannual variability in the North Atlantic Ocean carbon sink, *Science*, *298*, 2374–2378.
- Gruber, N., et al. (2009), Oceanic sources, sinks, and transport of atmospheric  $\text{CO}_2$ , *Global Biogeochem. Cycles*, *23*, GB1005, doi:10.1029/2008GB003349.
- Ho, D. T., C. S. Law, M. J. Smith, P. Schlosser, M. Harvey, and P. Hill (2006), Measurements of air sea gas exchange at high wind speeds in the Southern Ocean: Implications for global parameterizations, *Geophys. Res. Lett.*, *33*, L16611, doi:10.1029/2006GL026817.
- Karl, D. M., and R. Lukas (1996), The Hawaii Ocean Time-series (HOT) program: Background, rationale and field implementation, *Deep Sea Res., Part II*, *43*, 129–156.
- Key, R. M., et al. (2015), Global Ocean Data Analysis Project, Version 2 (GLODAPv2), *ORNL/CDIAC-162, ND-P093*, Carbon Dioxide Inf. Anal. Center, Oak Ridge Natl. Lab., U.S. Dep. of Energy, Oak Ridge, Tenn., doi:10.3334/CDIAC/OTG.NDP093\_GLODAPv2.
- Khatiwala, S., et al. (2013), Global ocean storage of anthropogenic carbon, *Biogeosciences*, *10*, 4801–4831, 2169–2191, doi:10.5194/bg-10-4801-2169-2013.
- Ko, Y. H., K. Lee, P. D. Quay, and R. A. Feely (2014), Decadal (1994–2008) change in the carbon isotope ratio in the eastern South Pacific Ocean, *Global Biogeochem. Cycles*, *28*, 775–785, doi:10.1002/2013GB004786.
- Körtzinger, A., P. D. Quay, and R. E. Sonnerup (2003), The relationship between anthropogenic  $\text{CO}_2$  and the  $^{13}\text{C}$  Suess effect in the North Atlantic ocean, *Global Biogeochem. Cycles*, *17*(1), 1005, doi:10.1029/2001GB001427.
- Landschützer, P., et al. (2015), The reinvigoration of the Southern Ocean carbon sink, *Science*, *349*, 1221–1224, doi:10.1126/science.aab2620.
- Matear, R. J., and G. Holloway (1995), Modeling the inorganic phosphorus cycle of the North Pacific using an adjoint data assimilation model to assess the role of dissolved organic phosphorus, *Global Biogeochem. Cycles*, *9*, 101–119, doi:10.1029/94GB03104.
- Matsumoto, K., et al. (2004), Evaluation of ocean carbon cycle models with data-based metrics, *Geophys. Res. Lett.*, *31*, L07303, doi:10.1029/2003GL018970.
- McNeil, B. I., R. J. Matear, and B. Tilbrook (2001), Does carbon-13 track anthropogenic  $\text{CO}_2$  in the Southern Ocean?, *Global Biogeochem. Cycles*, *15*, 597–613, doi:10.1029/2000GB001352.
- Mikaloff Fletcher, S. E., et al. (2007), Inverse estimates of the oceanic sources and sinks of natural  $\text{CO}_2$  and the implied oceanic carbon transport, *Global Biogeochem. Cycles*, *21*, GB1010, doi:10.1029/2006GB002751.
- Munro, D. R., N. S. Lovenduski, B. B. Stephens, T. Newberger, K. R. Arrigo, T. Takahashi, P. D. Quay, J. Sprintall, N. M. Freeman, and C. Sweeney (2015), Estimates of net community production in the Southern Ocean determined from time series observations (2002–2011) of nutrients, dissolved inorganic carbon, and surface ocean  $\text{pCO}_2$  in Drake Passage, *Deep Sea Res., Part II*, *114*, 49–63, doi:10.1016/j.dsr2.2014.12.014.
- Murata, A., Y. Kumamoto, S. Watanabe, and M. Fukasawa (2007), Decadal increases of anthropogenic  $\text{CO}_2$  in the South Pacific subtropical ocean along  $32^\circ\text{S}$ , *J. Geophys. Res.*, *112*, C05033, doi:10.1029/2005JC003405.
- Murata, A., Y. Kumamoto, Y. Sasaki, K. Watanabe, S., and M. Fukasawa (2009), Decadal increases of anthropogenic  $\text{CO}_2$  along  $149^\circ\text{E}$  in the western North Pacific, *J. Geophys. Res.*, *114*, C04018, doi:10.1029/2008JC004920.
- Olsen, A., et al. (2016), The Global Ocean Data Analysis Project version 2 (GLODAPv2) – an internally consistent data product for the world ocean, *Earth Syst. Sci. Data*, *8*, 297–323, doi:10.5194/essd-8-297-2016.
- Orr, J. C. (2002), Global ocean storage of anthropogenic carbon, final report, *Environ. and Clim. Programme*, Eur. Comm., Brussels. [Available at <http://www.ipsl.jussieu.fr/OCMIP/>]
- Plancherel, Y., K. B. Rodgers, R. M. Key, A. R. Jacobson, and J. L. Sarmiento (2009), Role of regression model selection and station distribution on the estimation of oceanic anthropogenic carbon change by eMLR, *Biogeosciences*, *10*, 4801–4831, doi:10.5194/bg-10-4801-2013.
- Quay, P., R. Sonnerup, J. Stutsman, J. Maurer, A. Kortzinger, X. Padin, and C. Robinson (2007), Anthropogenic  $\text{CO}_2$  accumulation rates in the North Atlantic Ocean from changes in the  $^{13}\text{C}/^{12}\text{C}$  of dissolved inorganic carbon, *Global Biogeochem. Cycles*, *21*, GB1009, doi:10.1029/2006GB002761.
- Quay, P. D., R. E. Sonnerup, T. Westby, J. Stutsman and A. P. McNichol (2003), Anthropogenic changes of the  $^{13}\text{C}/^{12}\text{C}$  of dissolved inorganic carbon in the ocean as a tracer of  $\text{CO}_2$  uptake, *Global Biogeochem. Cycles*, *17*(1), 1004, doi:10.1029/2001GB001817.
- Quay, P. D., J. Stutsman, R. A. Feely, and L. W. Juranek (2009), Net community production rates across the subtropical and equatorial Pacific Ocean estimated from air-sea  $\delta^{13}\text{C}$  disequilibrium, *Global Biogeochem. Cycles*, *23*, GB2006, doi:10.1029/2008GB003193.
- Sabine, C. L., and T. Tanhua (2010), Estimation of anthropogenic  $\text{CO}_2$  inventories in the ocean, *Annu. Rev. Mar. Sci.*, *2*, 175–198, doi:10.1146/annurev-marine-120308-080947.
- Sabine, C. L., R. A. Feely, F. J. Millero, A. G. Dickson, C. Langdon, S. Mecking, and D. Greeley (2008), Decadal changes in Pacific carbon, *J. Geophys. Res.*, *113*, C07021, doi:10.1029/2007JC004577.
- Sarmiento, J. L., and E. T. Sundquist (1992), Revised budget for the oceanic uptake of anthropogenic carbon dioxide, *Nature*, *356*, 589–593.
- Siegenthaler, U., and J. L. Sarmiento (1993), Atmospheric carbon dioxide and the ocean, *Nature*, *365*, 119–125.
- Sonnerup, R. E., and P. D. Quay (2012),  $^{13}\text{C}$  constraints on ocean carbon cycle models, *Global Biogeochem. Cycles*, *26*, GB2014, doi:10.1029/2010GB003980.
- Sonnerup, R. E., P. D. Quay, and A. P. McNichol (2000), The Indian Ocean  $^{13}\text{C}$  Suess effect, *Global Biogeochem. Cycles*, *14*(903-916), 2000.
- Takahashi, T., et al. (2009), Climatological mean and decadal change in surface ocean  $\text{pCO}_2$ , and net sea-air  $\text{CO}_2$  flux over the global oceans, *Deep Sea Res., Part II*, *56*, 554–577.

- Toggweiler, J. R., K. Dixon, and K. Bryan (1989), Simulations of radiocarbon in a coarse-resolution world ocean model 1: Steady state pre bomb distributions, *J. Geophys. Res.*, *94*, 8217–8242, doi:10.1029/JC094iC06p08217.
- Wakita, M., S. Watanabe, A. Murata, N. Tsurushima, and M. Honda (2010), Decadal change of dissolved inorganic carbon in the subarctic western North Pacific Ocean, *Tellus B*, *62*, 608–620, doi:10.1111/j.1600-0889.2010.00476.x.
- Wallace, D. W. R. (1995), Monitoring global ocean carbon inventories, rep., 54 pp. *Ocean Obs. Syst. Dev. Panel*, Texas A&M Univ., College Station, Tex.
- Waters, J. F., F. J. Millero, and C. L. Sabine (2011), Changes in South Pacific anthropogenic carbon, *Global Biogeochem. Cycles*, *25*, GB4011, doi:10.1029/2010GB003988.
- Weiss, R. F. (1974), Carbon dioxide in water and seawater: The solubility of a non-ideal gas, *Mar. Chem.*, *2*, 203–215.
- Williams, N. L., R. A. Feely, C. L. Sabine, A. G. Dickson, J. H. Swift, L. D. Talley, and J. L. Russell (2015), Quantifying anthropogenic carbon inventory changes in the Pacific sector of the Southern Ocean, *Mar. Chem.*, *174*, 147–160.
- Zhang, J., P. D. Quay, and D. O. Wilbur (1995), Carbon isotope fractionation during gas-water exchange and dissolution of CO<sub>2</sub>, *Geochim. Cosmochim. Acta*, *59*, 107–114.